Geophysical Journal International

Geophys. J. Int. (2012) **191,** 1025–1047 doi: 10.1111/j.1365-246X.2012.05692.x

Chemical and magnetic properties of rapidly cooled metastable ferri-ilmenite solid solutions: implications for magnetic self-reversal and exchange bias—III. Magnetic interactions in samples produced by Fe–Ti ordering

Peter Robinson,[1,2] R. J. Harrison,[3] Karl Fabian[1] and Suzanne A. McEnroe[2,4]

[1] *Geological Survey of Norway,* N-7491 *Trondheim, Norway. E-mail: peter.robinson@ngu.no*
[2] *Bayerisches Geoinstut, Universität Bayreuth,* D95440 *Bayreuth, Germany*
[3] *Department of Earth Sciences, University of Cambridge, Cambridge* CB2 3EQ, *UK*
[4] *Norwegian University of Science and Technology,* N-7491 *Trondheim, Norway*

Accepted 2012 September 24. Received 2012 September 24; in original form 2012 June 12

SUMMARY

Paper II of this series described the chemical and microstructural evolution of ferri-ilmenite solid solutions during high-*T* quench and short-term annealing. Here we explore consequences of these Fe–Ti ordering-induced microstructures and show how they provide an explanation for both self-reversed thermoremanent magnetization and room-*T* magnetic exchange bias. The dominant antiferromagnetic interactions between (001) cation layers cause the net magnetic moments of ferrimagnetic ordered phases to be opposed across chemical antiphase domain boundaries. Magnetic consequences of these interactions are explored in conceptual models of four stages of microstructure evolution, all having in common that A-ordered and B-anti-ordered domains achieve different sizes, with smaller domains having higher Fe-content, lesser Fe–Ti order, and slightly higher Curie *T* than larger domains. Stage 1 contains small Fe-rich domains and larger Ti-rich domains separated by volumes of the disordered antiferromagnetic phase. Magnetic linkages in this conceptual model pass through disordered host, but self-reversed TRM could occur. In stage 2, ordered domains begin to impinge, but some disorder remains, creating complex magnetic interactions. In stages 3 and 4, all disordered phase is eliminated, with progressive shrinkage of Fe-rich domains, and growth of Ti-rich domains. Ordered and anti-ordered phases meet at chemical antiphase and synphase boundaries. Strong coupling across abundant antiphase boundaries provides the probable configuration for self-reversed thermoremanent magnetization. Taking the self-reversed state into strong positive fields provides a probable mechanism for room-temperature magnetic exchange bias.

Key words: Magnetic mineralogy and petrology; Reversals: process, time scale, magnetostratigraphy; Rock and mineral magnetism.

1 INTRODUCTION

Paper I of this series (Fabian *et al.* 2011) gave a detailed description of chemical microstructures and magnetic features of a synthetically quenched ferri-ilmenite sample of composition X $FeTiO_3$ = 0.61, as well as magnetic properties produced in this sample by short-term annealing. An overview was given of available studies on similar natural and synthetic samples in relation to theories of self-reversed thermoremanent magnetization (TRM) and magnetic exchange bias. In Paper II (Robinson *et al.* 2012) an analysis was presented of the chemical phase relations and processes leading to the microstructures considered most favourable to produce these magnetic properties, as previously proposed by Harrison *et al.* (2005) and Harrison (2006). In Paper II it was shown that 'contact layers', previously shown to be the key to 'lamellar magnetism' in exsolved intergrowths of near end-member hematite and ilmenite (Harrison & Becker 2001; Robinson *et al.* 2002, 2004; Fabian *et al.* 2008; McCammon *et al.* 2009), also apply at interfaces between disordered, ordered and anti-ordered solid solutions of essentially the same composition.

Details of the chemical ordering process, covered in Paper II, can be divided into two aspects that are summarized briefly here. When a disordered phase starts to order, isolated Fe–Ti ordered and Ti–Fe anti-ordered domains appear, producing a complex microstructure. With further development, these domains grow and antiphase boundaries (APBs) appear, which themselves contain a degree of disorder. Experiments and TEM imaging of Nord & Lawson (1989) proved that annealing causes coarsening of these quench microstuctures and gradual elimination of APB's. However, due to equilibrium entropy, absence of microstructure does not imply complete order.

Order in the solid solution is described by the order parameter Q, ranging from 0 (complete disorder) to 1 (perfect order). This has been studied in powder neutron diffraction experiments at temperature (T) by Harrison & Redfern (2001), where the different neutron diffraction properties of Fe and Ti allow direct measurement of Q for a sample. Thermal runs began at low T with a quenched sample with microstructure, where results averaged everything. As T rose, at first average Q increased due to microstructure annealing, then declined due to the entropy at thermal equilibrium, eventually reaching 0 at high T, indicating a homogeneous disordered phase. In subsequent slow cooling, Q increased and in a few runs reached $\sim$0.9 at low T. Here, without unrealistically long and slower cooling, ordering shuts down and perfect order is not obtained. In Paper I we described a sample of Ilm 61.8 which was held at 685 °C below the disorder-order temperature for 39 months before quench and still retains $Q \sim 0.64$. Magnetic studies suggested this sample lacked microstructure, but its ordered phase showed the equilibrium degree of disorder appropriate to the temperature it had been held at.

A key feature of the ferri-ilmenite part of this solid solution series, as contrasted with the titanohematite part, is that virtually all chemical processes are completed at temperatures (T) well above those where magnetic interactions occur (Burton *et al.* 2008), thus making it possible to separate the chemical processes discussed in Paper II, from magnetic processes described here in Paper III. Here, the details of the microstructures previously described are coupled with well-known magnetic interactions in this series (Ishikawa *et al.* 1985; Harrison 2006; Robinson *et al.* 2010) to create graphic models that provide a sound qualitative explanation of both self-reversed TRM, and room-T magnetic exchange bias. Actual routes to obtain materials in which these properties are optimal will only be discovered through an organized program of controlled syntheses and annealing followed by magnetic experiments. An important start on such a program was made by Lagroix *et al.* (2004) using several $X = 0.70$ samples quenched by Nord & Lawson (1989) with results of some pertinence to what we say below. We are currently embarked on a wider program for $X = 0.60$, 0.65 and 0.70 with various temperatures of quench and annealing.

The paper begins by describing the nature of magnetic interactions in these mixed-phase assemblages, taking account of the detailed nature of phase interfaces. We then discuss the progressive acquisition of magnetization on cooling in both weak and strong magnetic fields, and compare the behaviour of materials with different degrees of chemical order, which result from different quench and annealing conditions. We discuss in detail the specific chemical and magnetic interface conditions in intergrowths that are partially ordered, but divided into ordered and anti-ordered domains of different sizes. Finally we demonstrate how such intergrowths may explain both self-reversed TRM and room-T exchange bias.

2 TERMINOLOGY FOR CHEMICAL AND MAGNETIC DOMAINS AND INTERACTIONS ACROSS THEIR BOUNDARIES

2.1 Room-T coupling of antiferromagnetic and ferrimagnetic phases

The simplest magnetic interactions of disordered and ordered rhombohedral oxides are discussed by considering a disordered antiferromagnetic host which is magnetically analogous to hematite (Ishikawa *et al.* 1985; Harrison 2006; Nabi *et al.* 2010; Robinson *et al.* 2010), though substituted with significant Fe^{2+} and Ti^{4+} in random distribution. The magnetic superexchange interactions between alternate layers parallel to (001) are antiferromagnetic, which means that each sublattice magnetization, averaging 3.2 μB for Ilm 60, has a magnetic moment that is essentially antiparallel to the magnetic moments within adjacent layers. The same antiferromagnetic relationship between layers appears in all the individual model blocks in Fig. 1.

An entire assemblage of disordered layers has a net magnetic moment of essentially zero in the direction of the sublattice magnetizations, but a very slight moment in the (001) plane at right angles to the sublattice magnetization directions because these are a very small fraction of one degree out of perfect antiparallel orientation. This gives rise to the so-called 'spin-canted' magnetization of hematite, which is deeply involved in several proposed models for self-reversed TRM as discussed in Paper I (Fabian *et al.* 2011). However, the calculated net magnetic moment for the spin-canted magnetization for this composition, assuming the same canting angle as observed in pure hematite, would be 0.0073 μB pfu, which is miniscule compared to the sublattice magnetization, and also compared to the net ferrimagnetic moment of fully ordered Ilm 60 which is 2.4μ_B pfu.

When Fe–Ti ordered and Ti–Fe anti-ordered phases develop within a disordered matrix at high T, they will be of either the A-type, or the B-type. For purposes of modelling here, we define order A as having Fe-rich layers located at the top of a model block, and order B as having Fe-rich layers in the second layer below the top of a model block as in Fig. 1. Even though having sublattice magnetic orientations compatible with their disordered hosts, the ordered phases, unlike their host, will have a significant net magnetic moment created by the fact that the iron-rich layers have a higher magnetic moment than the Ti-rich layers, and the order A and order B layers will also have opposite magnetic moments due to opposite placement of Fe-rich layers. For perfectly ordered composition Ilm 60, the Fe-layer has a moment of 4.4 μB and the Ti layer 2 μB, giving the net moment 2.4 μB, however, in natural situations, the Ti-order parameter Q (Robinson *et al.* 2012) will not attain this perfect order ($Q = 1$) and net magnetic moments can be far lower.

When A-ordered and B-anti-ordered phases impinge during intergrowth coarsening, with progressive elimination of the disordered phase, they impinge along chemical antiphase domain boundaries (CAPB). In addition, interfaces have been identified (Robinson *et al.* 2012) where two impinging phases have the same chemical ordering scheme, but nevertheless different degrees of Fe-enrichment. These are termed chemical synphase domain boundaries (CSPB).

2.2 Graphic key to magnetic interactions across chemical phase boundaries

Before exploring acquisition of magnetization in samples dominated by chemical domain boundaries, we examine the

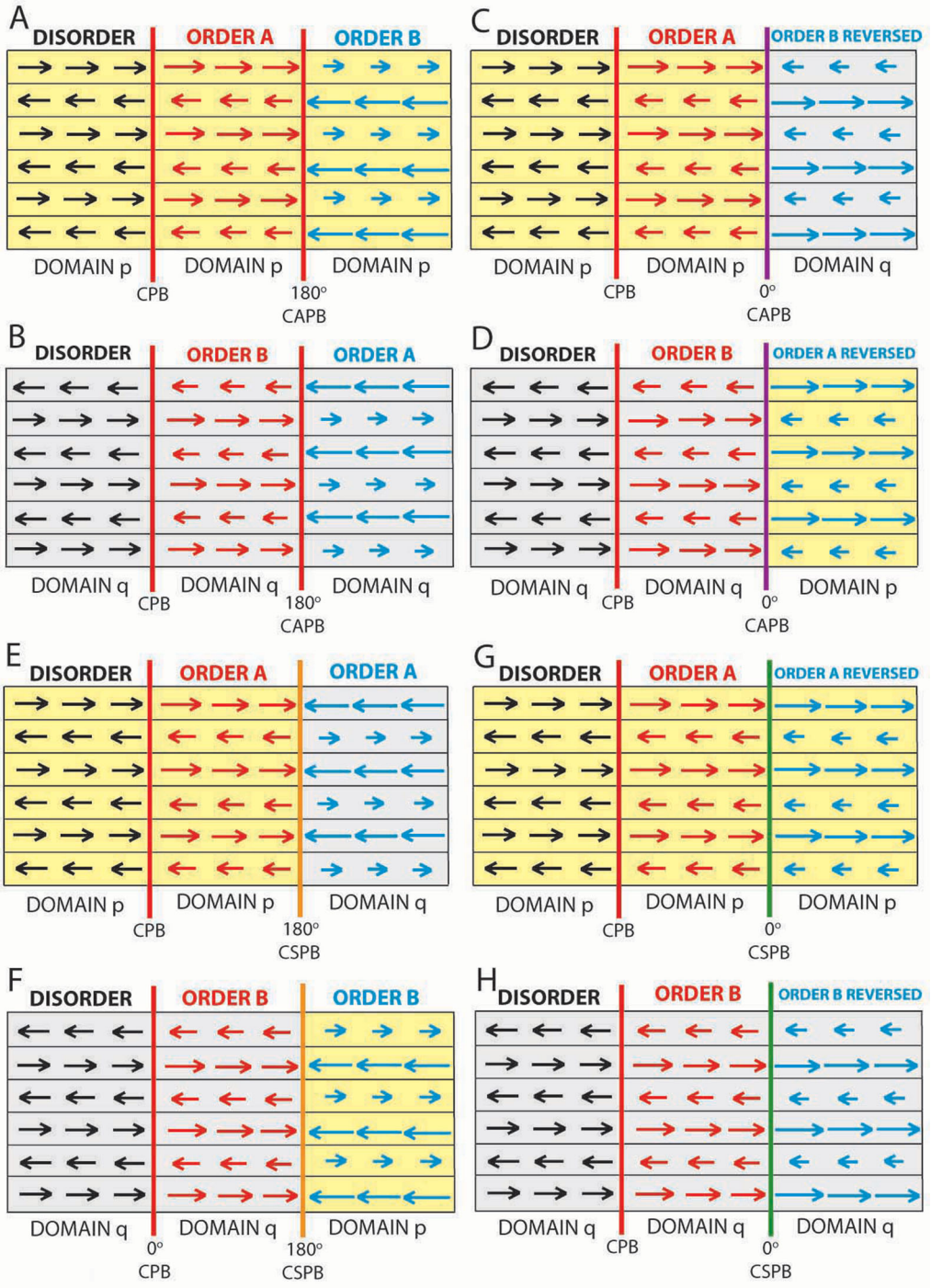

Figure 1. Template for understanding chemical and magnetic relations between disordered domains and different ordered domains under varied magnetic conditions and locations as portrayed in Figs 2–6 and 10. Abbreviations for domain boundaries: CPB, chemical phase boundary; CAPB, chemical antiphase boundary; CSPB, chemical synphase boundary. For other explanations see text.

characteristics and terminology of the boundaries themselves. Each of eight panels A–H in Fig. 1 begins on the left with a disordered block of layers denoted by magnetic sublattice arrows of equal length implying no net magnetic moment. When the arrows in the top layer in the block point to the right, this is described as a 'p domain' and shaded yellow; when the arrow in the top layer points to the left, this is described as a 'q-domain' and shaded grey. This dual classification of sublattice orientations holds throughout all the panels, regardless of placement of Fe-layers or net magnetic moments in ordered and anti-ordered phases. This 'p' and 'q' terminology and colour scheme is used in all the graphic models to follow.

To the right of the disordered blocks there are order A and order B blocks. In these the lengths of the magnetic sublattice arrows are schematically proportional to Fe-content, so that the directions of the longer Fe-rich arrows indicate the directions of the net ferrimagnetic moments. In the red central blocks, the degree of order is considered less, and total Fe content more, leading to a weaker net magnetic moment but a higher Curie T, meaning that red blocks

should magnetize first in a cooling sequence. This is symbolized by a lesser difference in length of sublattice arrows. In the blue right-hand blocks, the degree of order is considered greater, and total Fe content less, leading to a stronger net magnetic moment, but a lower Curie T, meaning that blue blocks should magnetize later in a cooling sequence. This is symbolized by a greater difference in length of sublattice arrows. In all the panels the red central blocks are considered to magnetize first with a net magnetic moment directed to the right parallel to a positive field directed to the right. Directions of net magnetic moments of the blue blocks depend on strength of antiferromagnetic interactions across the phase boundaries in competition with the strength of the applied magnetic field.

Panel A shows a red order A block compatibly linked to a disordered block, and to a blue anti-order B block. All are magnetically compatible within a 'p domain', but A and B show opposite net moment directions. Panel B is like panel A, except it shows a red order B region compatibly linked to a blue anti-order B region. Here all are magnetically compatible within a 'q domain' but again A and B show opposite net moment directions. Panels A and B contain the main essentials for self-reversed TRM. The boundaries between A and B domains in red are chemical APBs with net magnetic moments at 180°, hence labelled '180° CAPB'. The boundaries between disordered and A or B domains are also marked red in all the panels, but these are not APBs in the standard sense, only chemical phase boundaries (CPB).

Panels C and D illustrate what happens with imposition of a strong positive field to the right to the situations in panels A and B. This reverses the net magnetizations of the blue blocks and creates new domain p, and domain q sublattice arrangements. The net magnetic moment arrangements across the boundaries in violet are now parallel. Therefore, these chemical APBs with net magnetic moments at 0° are here labelled '0° CAPB', and they are energetically unfavourable. This is because the sublattice magnetization arrows across A–B domain boundaries are out of phase, meaning that the normal antiferromagnetic interactions within the blocks do not take place across the interface. The situation illustrated in panels C and D can arise either by application of a strong field at room temperature or by application of a strong enough field during cooling as illustrated by Lagroix *et al.* (2004) in their fig. 8.

Panel E shows the results when a red order A block impinges on blue order A block on the boundaries between domains later to become large p and q domains within a coarsening intergrowth (see Figs 5 and 6 below). The blue block has an opposite net magnetic moment from the red block, also reflected in the p–q magnetic domain boundary. Panel F shows the same when a red order B block impinges on a blue order B block on the same kind of p–q boundary. These are initially chemical boundaries, but different in nature from the APBs illustrated in Panels A and B. Here the adjacent ordered regions have the same chemical position of the Fe- and Ti-rich layers, and differ only in the degree of ordering and composition, with the red regions less ordered and more Fe-rich than the blue regions. To describe these, we created the term 'synphase boundaries' (Robinson *et al.* 2012). The boundaries in panels E and F in orange are therefore chemical synphase boundaries (CSPB) with net magnetic moments at 180°, hence labelled '180° CSPB', and here they are also boundaries between p and q domains. Across a 180° CSPB the magnetic interlayer interactions are not antiferromagnetic and hence energetically unfavourable.

Panels G and H illustrate what happens with imposition of a strong positive field to the right to the situations in panels E and F, which reverses the magnetizations of the blue blocks. This creates new sublattice domain arrangements, all domain p in panel G, and all domain q in panel H. However, the net magnetic moment arrangements across the boundaries in green are parallel. Therefore, these CSPB with net magnetic moments at 0° are here labelled '0° CSPB'. These 0° CSPB boundaries, now become energetically favourable with normal antiferromagnetic interlayer interactions across domain interfaces.

There is an important difference between lower-energy phase boundaries that preserve antiferromagnetic interactions and lie entirely in p or q domains, and higher-energy boundaries that lie on p–q domain walls. Panels A, B, G and H show the former; panels C, D, E and F show the latter. The magnetic importance of the changes in going from panels E and F to G and H, are discussed in conjunction with Fig. 10.

Fig. 1 was created in 2009. The message to be taken and carried forward from it by the reader is remarkably encapsulated in a phrase from a long poem by Charles Churchill, published 1763 (found by us in 2012), from which we provide the following excerpt (Oxford English Dictionary, 2007 Edition). 'On all occasions next the chair, He stands for service of the Mayor, And to instruct him how so use, His A's and B's, and P's and Q's'.

2.3 Magnetization near interfaces between disordered, ordered and anti-ordered phases

The images in Fig. 2 show that there are two different microstructures to be considered in these samples: (1) a static chemical microstructure defined by the A-ordered, B-anti-ordered and disordered regions (Fig. 2A) and (2) a mobile microstructure that is determined by the distribution of p and q sublattice domains (Figs 2B, C and D). The boundary between p and q sublattice domains in all cases is simply a Bloch wall, where the sublattice spins rotate through 180°. This fact never changes. However, the magnetic character of the Bloch wall does change according to whether the wall sits inside an ordered domain, inside a disordered region, on an antiphase boundary or on a synphase boundary. In different applied fields, the Bloch walls move, and will adopt different configurations to achieve the minimum energy state. In a weak magnetic field, such an energy state will be one with the minimum abundance of magnetic Bloch walls consistent with the distribution of prior imposed chemical walls.

The static chemical microstructure illustrated in Fig. 2(A) consists of A-ordered and B-ordered domains within a disordered matrix with the relevant array of 'contact layers' as described in Paper II. Fig. 2(B) illustrates the magnetic structure obtained when the entire region forms part of a uniform p sublattice domain. The A and B domains have oppositely directed net ferrimagnetic moments, as shown by the large red and blue arrows. The reversal of net magnetization occurs at the chemical APBs, producing what Harrison *et al.* (2005) called a '180° chemical domain wall' or 180° CAPB in present notation. The wall is defined by chemistry imposed at higher T, but the 180° reversal of the net ferrimagnetic moment occurs because the two domains are chemically out of phase. Although the magnetizations described in Fig. 2(B) are portrayed as spontaneous, the same pattern would result if the red A-ordered region, being more Fe-rich, were magnetized first in cooling in a relatively weak magnetic field applied horizontally to the right.

Domain walls of different character are derived if a strong positive magnetic field is applied progressively as in Figs 2(C) and (D), so that by 2(D) all the negatively magnetized B regions have acquired a positive magnetization, overcoming the magnetic exchange

coupling along the A–B chemical domain boundary (see Lagroix *et al.* 2004, Fig. 8). This magnetic reversal is achieved by nucleating a q sublattice domain on the right hand side (Fig 2C), and then driving the resulting p–q Bloch wall through the B-ordered region until it fully decorates the chemical antiphase boundary (Fig. 2D). This produces what Harrison *et al.* (2005) called a '0^o magnetic antiphase domain wall' or 0° CAPB in present notation, marked in violet in Figs 2(C) and (D). The existence of 0° magnetic walls decorating APBs in quenched and annealed ferri-ilmenite has been identified using electron holography (Harrison *et al.* 2005). While the p–q Bloch wall still resides within the interior of an A-ordered or B-ordered domain it acts as a conventional '180^o magnetic wall' (marked blue in Fig. 2C). When the p–q Bloch wall resides entirely within the disordered phase (left hand side of Fig. 2D), it might more accurately be described as a 180° antiferromagnetic wall. The former were observed directly in electron holography of a sample of quenched and annealed Ilm 70 by Harrison *et al.* (2005).

Differences in domain wall types are critical in understanding magnetic behaviour, and additional types were needed (see Fig. 1) for full behaviour description. The domain walls illustrated in Figs 2(B)–(D) are shown schematically in that they have no thickness, whereas true domain walls would have a thickness of a number of atomic layers depending on their character. Using electron holography, Harrison *et al.* (2005) estimated the widths of domain walls: 19 nm for 180^o magnetic walls, 7 nm for 180^o CAPBs and 50 nm for 0^o CAPBs.

3 MECHANISM FOR MAGNETIC SELF-REVERSAL

3.1 General features

The mechanism for magnetic self-reversal requires an intergrowth of two materials with different Curie T's: a minor phase, which acquires a magnetization at higher T; and a major phase, or at least one with a more intense magnetization, that acquires a magnetization at a lower T. Most early workers (Uyeda 1957, 1958; Ishikawa 1958) were convinced that exchange coupling across phase interfaces was required for this process. Nevertheless, many subsequent papers (Hofmann 1975, 1992; Prévot *et al.* 2001) proposed models involving magnetostatic interactions of magnetic fields within the self-reversed material. Based on the room-T exchange bias loop published by Meiklejohn & Carter (1959) for a sample like the Haruna Dacite, and magnetic experiments by Ishikawa & Syono (1963), it seems to us quite certain that phase interface coupling is involved, as outlined above, and not magnetostatic interactions. Further it appears that the simple antiferromagnetic coupling between phases illustrated in Figs 1 and 2 is sufficient to achieve these results, even if the interface details may be complicated locally by contact layers.

A salient feature of nearly all materials showing magnetic self-reversal is the involvement of Fe–Ti ordering, necessarily combined with some kind of phase separation very similar to what we postulated for the Ilm 61 sample (Fabian *et al.* 2011). The experiments on an Ilm 70 composition by Nord & Lawson (1989, 1992) demonstrated, in a series of TEM photographs, the appearance of very fine antiphase domains after cooling through the disorder to order transition, the onset of magnetic self-reversal with some annealing, and major coarsening with further annealing, resulting in near elimination of the antiphase domains, and disappearance of the self-reversal process. Notably, unlike our quenched Ilm 61 sample, the experimental sample of Nord and Lawson, as well as the natural Haruna Dacite and Pinatubo samples, were all subject to annealing or cooling over a period longer than a few seconds. In addition to having this in common, they cover a considerable composition range from Ilm 75 down perhaps Ilm 46.5 (Uyeda, and Ishikawa and Syono experiments), all indicating the involvement of both a disorder to order transition and phase separation, much as we suggested in Paper II. The single exception to these common features is the study of a different Pinatubo sample by Hoffmann & Fehr (1996) who indicated that two compositions occur together along the contact between primitive cores and more chemically evolved rims of oxide phenocrysts.

3.2 Sample requirements for magnetic self-reversal

How then does the on-going annealing process produce the conditions for magnetic self-reversal not present in our original quenched Ilmenite 61 sample? The key lies in the proposal for the coarsening process made by Harrison *et al.* (2005) and Harrison (2006) based on a Monte Carlo simulation of coarsening of an Ilm 70 composition and accompanying magnetic holography experiments followed by a magnetic model indicating self-reversal at low T. This is supported by the evidence for self-reversal we obtained on our quenched Ilmenite 61 sample (Fabian *et al.* 2011), after short term annealing below the ordering T.

The annealing process begins with the situation similar to that illustrated for our quench sample in Fig. 3(A). The annealing process requires some parts of the crystal to become dominated by enlarged chemical A-ordered regions, with smaller B-anti-ordered regions. During this, the A-ordered regions also become poorer in Fe across a metastable chemical two-phase loop, whereas the smaller B-anti-ordered regions remain relatively richer in Fe (Robinson *et al.* 2012). While this is going on in some parts of the crystal, other parts become dominated by enlarged B-anti-ordered regions that become poorer in Fe and smaller A-ordered regions that remain relatively Fe-richer. It is possible that the total ordering process, with division of the crystal into A-dominant and B-dominant regions takes place in several sequential size steps as suggested by Harrison (2006).

For our purpose here, the theoretical results of different quenches and annealings are given in Figs 3(A), 4(A), 5(A) and 6(A), each representing the starting points of microstructure stages 1, 2, 3 and 4 in the progress of acquisition of magnetization. In Fig. 3(A) there is a disordered host, but Fe–Ti ordered and Ti–Fe anti-ordered domains are in two dominant size categories, small red and large blue, as a result of different locations and times of initiation and different growth rates. Fig. 4(A) is similar to Fig. 3(A) in containing significant disordered host, but the large blue ordered and anti-ordered domains have enlarged substantially so that they impinge on each other locally, and also very locally they impinge on small red ordered regions. In Fig. 5(A) all of the disordered host has been consumed so that ordered and anti-ordered domains impinge either along APBs or synphase boundaries. In addition, annealing has caused growth of the large (blue) ordered and anti-ordered domains, and shrinkage of small red ones. Those that shrank have acquired a higher Fe content and hence a higher magnetization T compared to those that grew in the progressive ordering process (Robinson *et al.* 2012). Fig. 6(A) represents a further step in the ordering process in which small red ordered regions have shrunk much more and are now nearly completely surrounded by large blue-ordered regions.

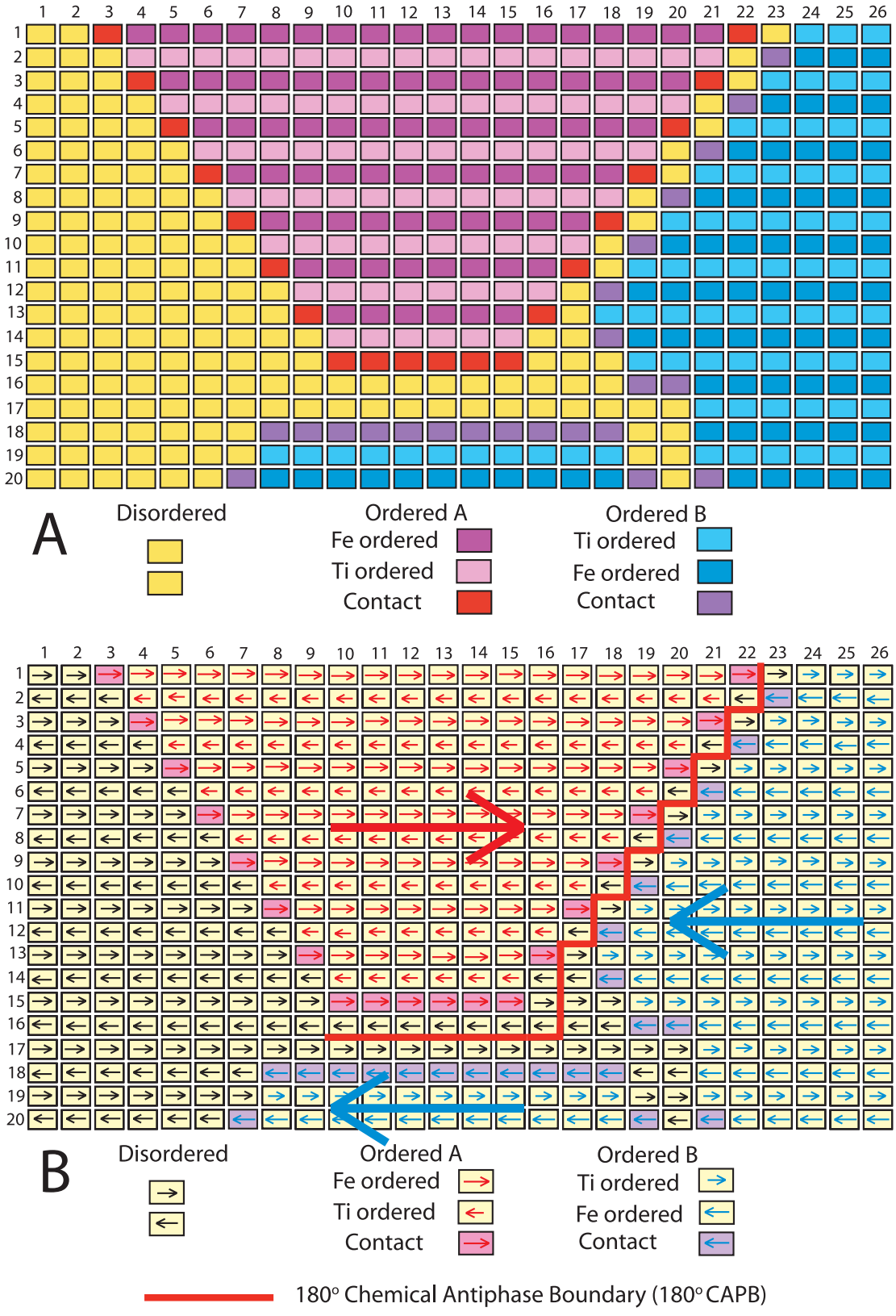

Figure 2. **(A)** Schematic diagram derivative from Paper II for Ilm 60 composition showing distribution of disordered solid solution (yellow), A-ordered regions (shades of red) and B-anti-ordered regions (shades of blue), as well as contact layers in red and violet, respectively. **(B)** The same chemical diagram as (A) but with all sublattice magnetizations shown schematically, assuming that the red A-ordered region was first magnetized as a ferrimagnet by a magnetic field directed horizontally to the right, and all other regions were then magnetized compatibly, indicated by yellow p-domain colour. The red A-ordered region thus shows a net ferrimagnetic moment to the right (large red arrow), the blue anti-ordered region shows a net ferrimagnetic moment to the left (large blue arrows) on the opposite sides of a 180° CAPB, and the disordered region is antiferromagnetic.

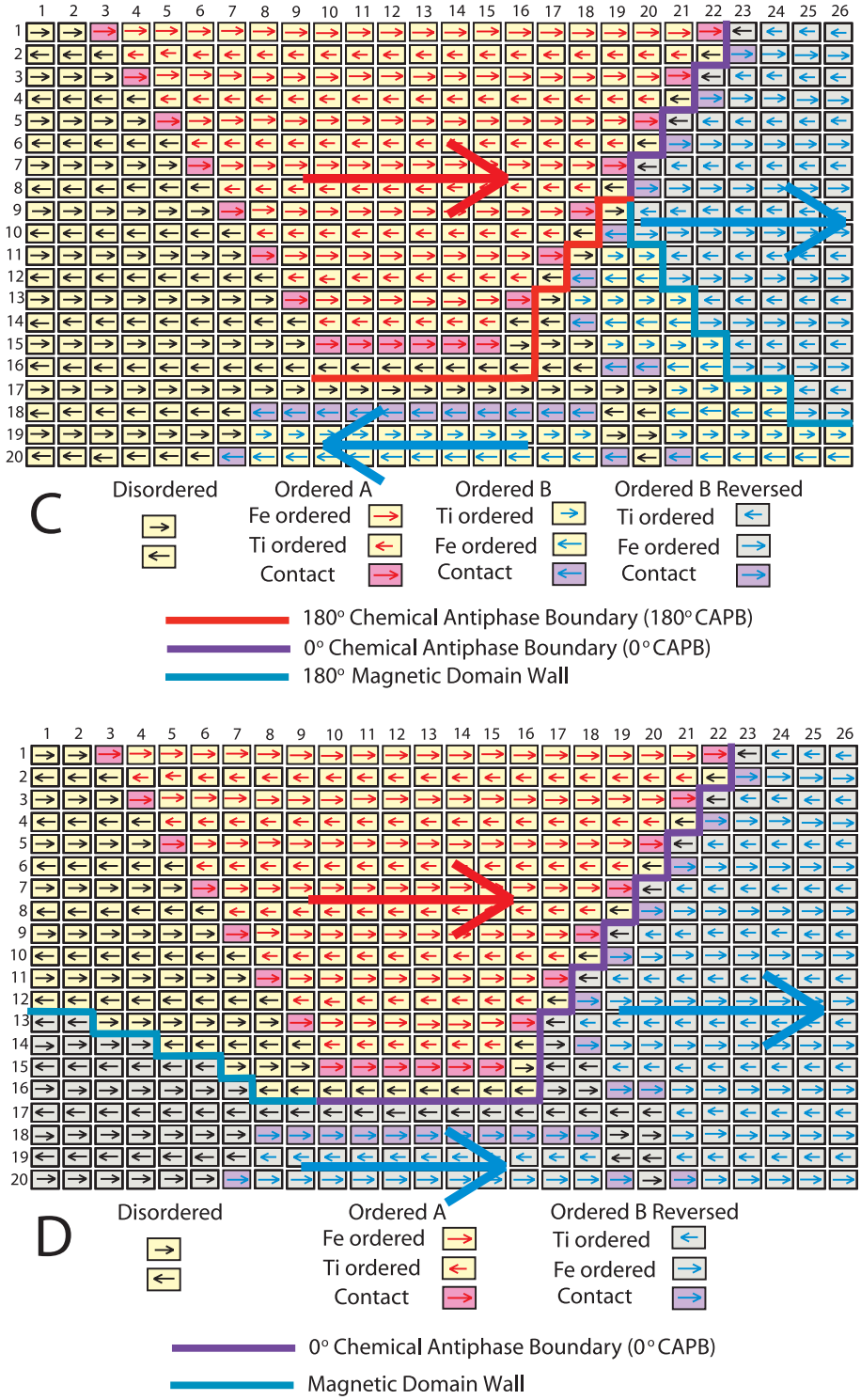

Figure 2. **(C)** The same material as (A) but magnetically different from (B) because the net magnetic moment direction of the upper right hand part of the ferrimagnetic B-anti-ordered region has been reversed by a stronger magnetic field to the right, so that its net moment is parallel to that of the A-ordered region (large blue arrow). The boundary between the two parts of the B-anti-ordered region is marked by a blue 180º magnetic wall, indicating opposite net magnetic moments of these two parts. The magnetically reversed region is also magnetically incompatible with the adjacent A-ordered and B-anti-ordered regions as indicated by a p–q domain boundary. Also, the magnetically reversed part of the B-anti-ordered region has a net moment 0º from the adjacent A-ordered region. The field has overcome the strong antiferromagnetic coupling across the 180° CAPB causing it to become a violet 0° CAPB. **(D)** The same material as (A) and magnetically similar to (C) except a stronger positive field has been applied. This caused all the B-anti-ordered domain to acquire a net magnetic moment to the right (large blue arrows) and also cause compatible magnetization to extend partially into the adjacent disordered matrix, indicated by spreading of the q domain over all of the B-anti-ordered region and part of the disordered region. The previous red 180° CAPB is now entirely replaced by a violet 0° CAPB. The previous blue 180º magnetic wall has moved entirely across the B-anti-ordered region and into the disordered antiferromagnetic region, where it can only be described as a magnetic wall because there is no net moment on either side. In the real cases, the magnetic boundaries are not single surfaces, as marked schematically here, but complex walls a few to many layers thick.

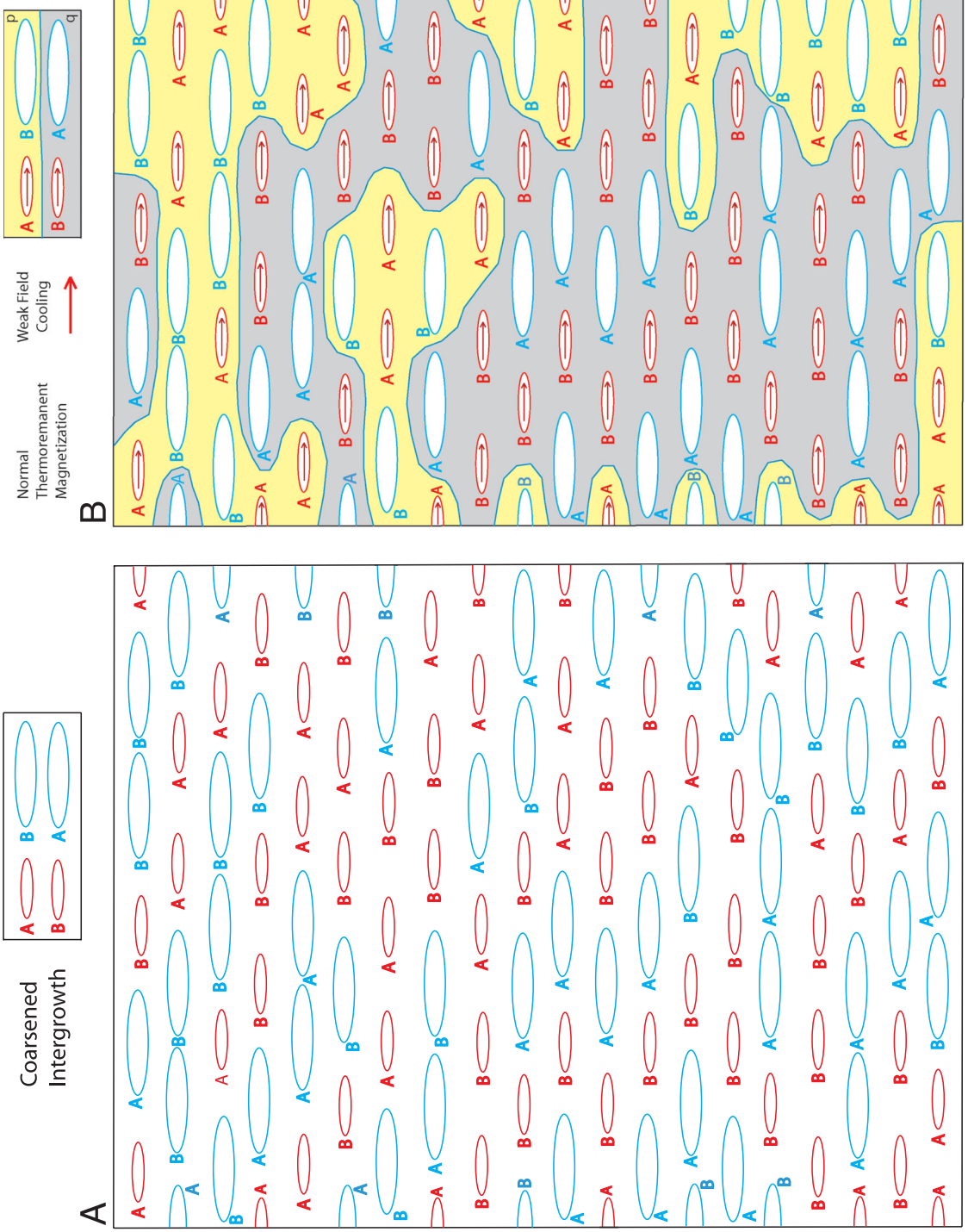

Figure 3. Qualitative model for microstructure stage 1 showing phase behaviour in a quenched and slightly annealed Ilm 60 sample. **(A)** Array of chemical domains after quench, consisting of A- and B-ordered domains in a disordered host. Domain colours and sizes, more or less randomly selected, determine the sequence by which magnetization occurs on cooling, where the smallest (red) ordered domains are considered to have the highest Fe content causing them to order first. **(B)** In a weak positive field to the right, the small red chemical A-ordered and B-anti-ordered domains have magnetized first, producing a weak normal ferromagnetic moment. Magnetization of red domains is also assumed to determine the magnetic sublattice arrangements in the antiferromagnetic disordered host, creating magnetic walls (blue lines) separating p and q domains.

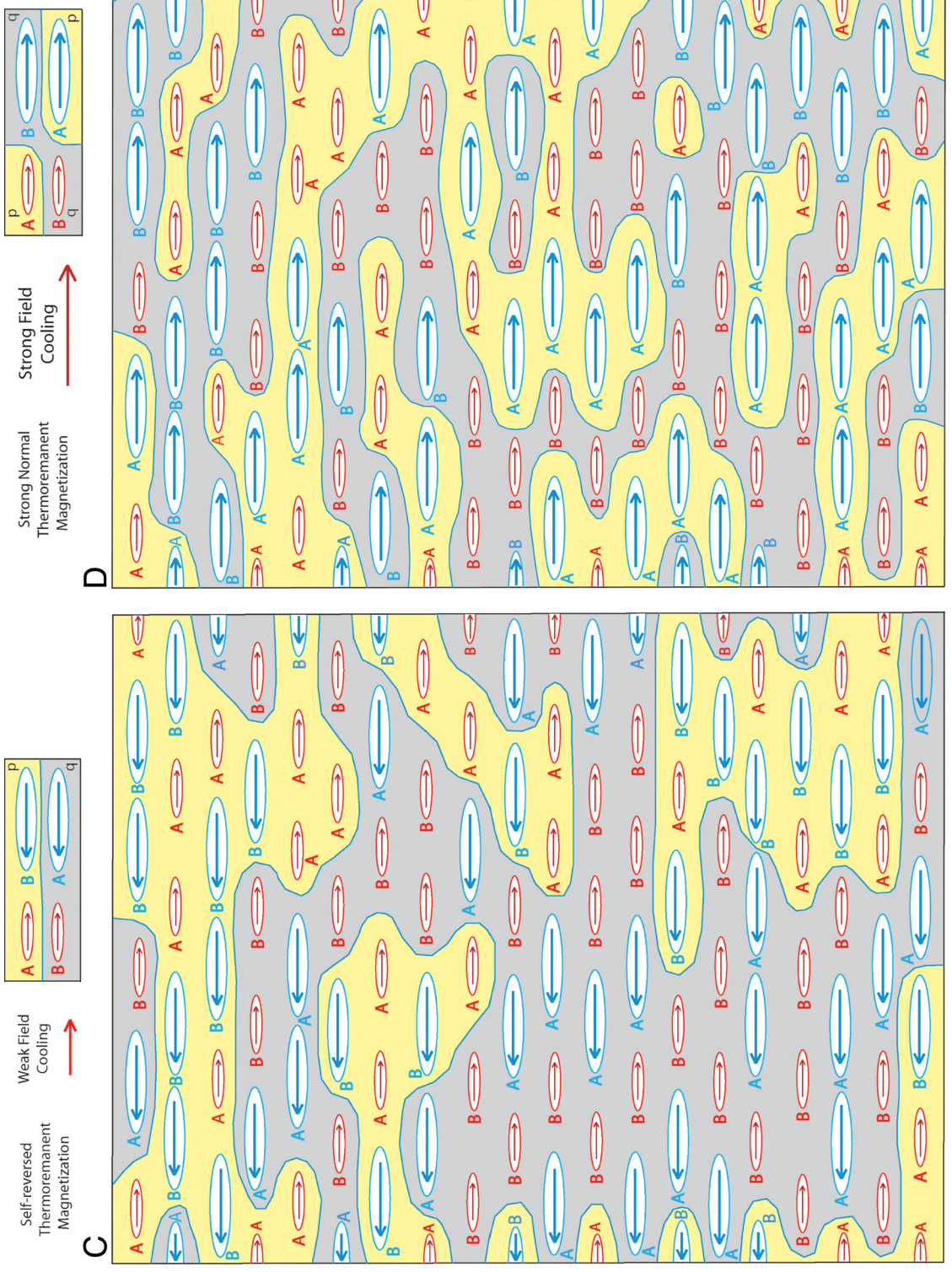

Figure 3. **(C)** Antiferromagnetic coupling to arrangements in 3B determines the magnetization orientations of the large Ti-richer (blue) domains at lower T, resulting in acquisition of self-reversed TRM. Reversed blue domains are more voluminous than red domains, and also have marginally higher magnetic moment because of better order and higher Ti content. **(D)** When cooled in strong magnetic field or when strong field is applied, situation in 3C is changed. All A- and B-ordered domains magnetize parallel to the field, creating a new, more extensive, hierarchy of magnetic walls (blue lines) and p and q arrangements within disordered host. Magnetic domain walls increase by 54 per cent between 3C and 3D.

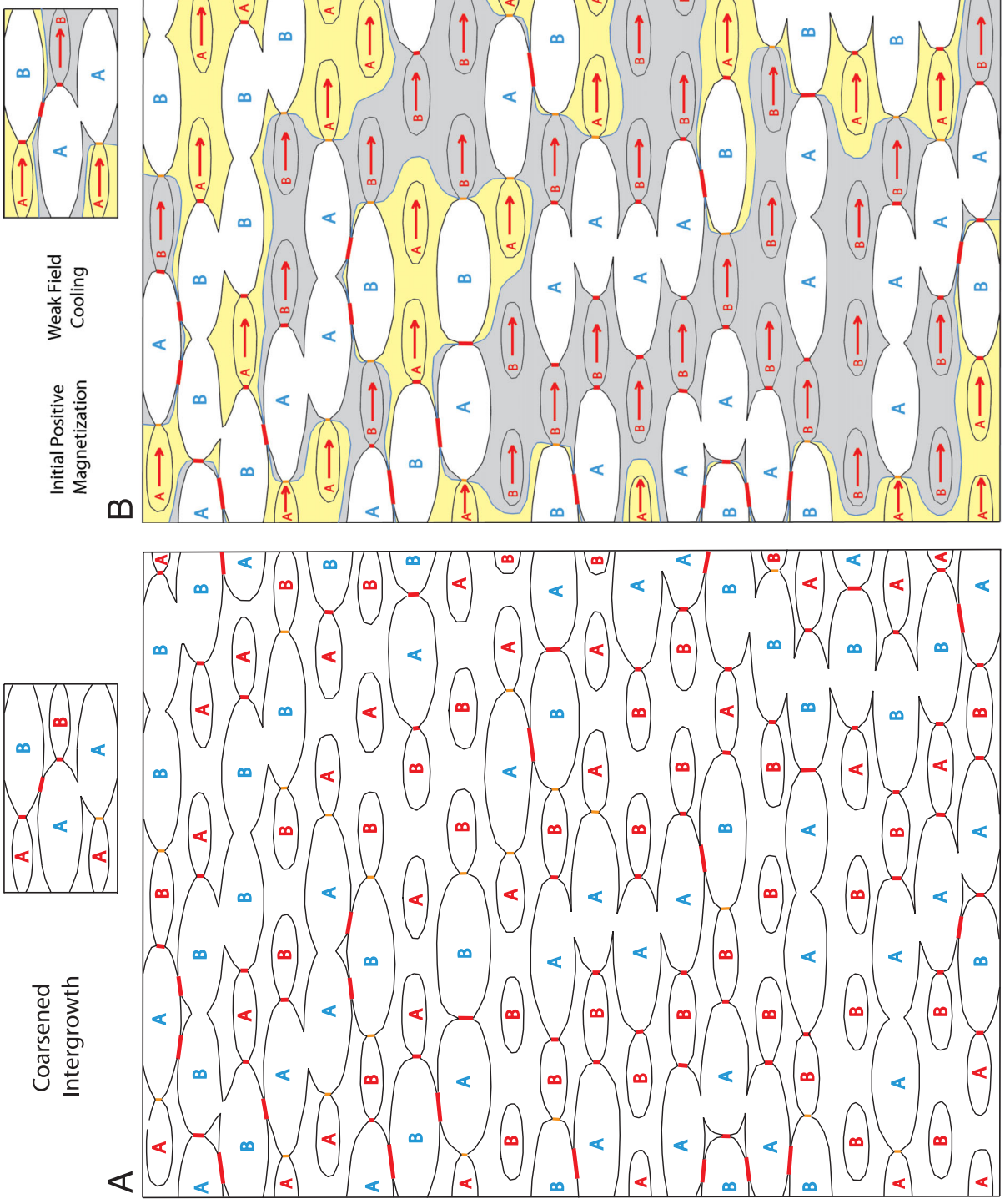

Figure 4. Sequence of magnetization acquisition for microstructure stage 2 in weak positive field to the right in stylized coarsened intergrowth of ordered and anti-ordered domains, where extensive disordered matrix remains, but there is partial impingement of ordered regions, creating CAPBs and CSPBs. **(A)** Diagonal impingement between large domains. Large domains impinge with small domains along (001). No impingement between small domains. **(B)** Initial magnetization of red ordered domains in positive field producing weak normal TRM and magnetically compatible p and q domains in disordered matrix. Neither CAPBs nor CSPBs are magnetic boundaries.

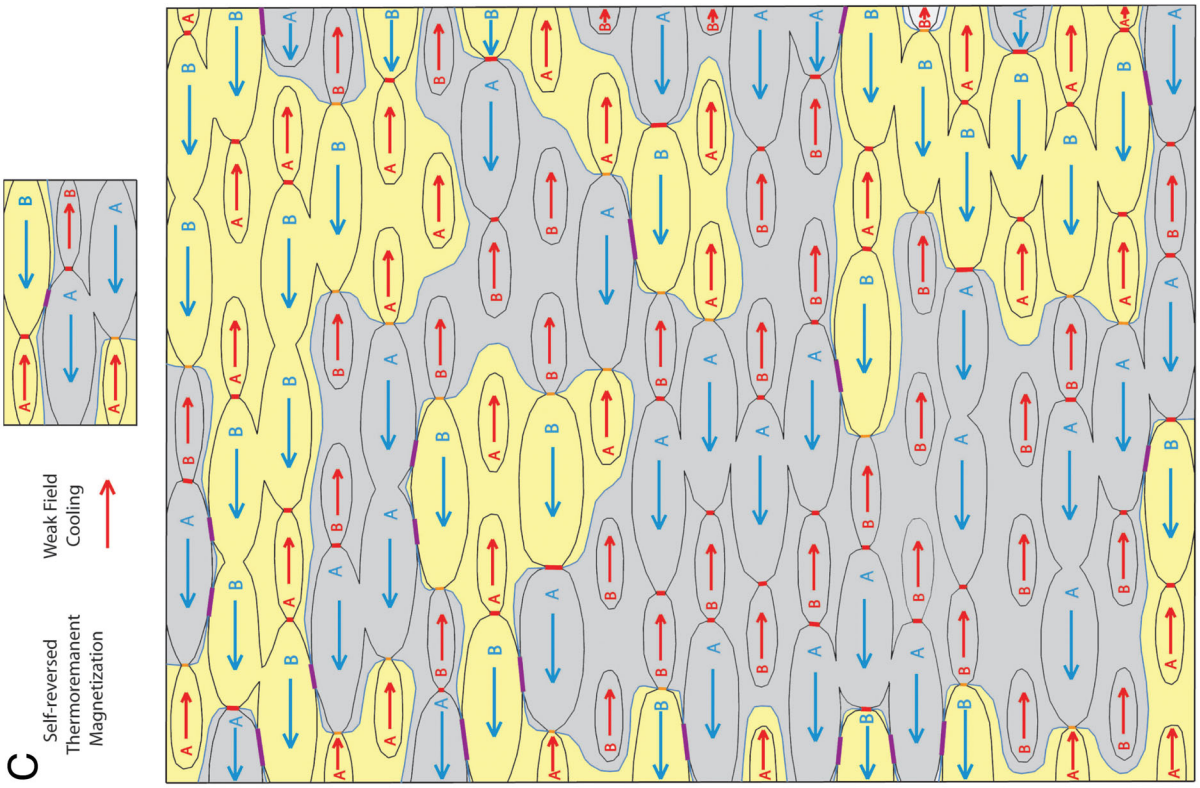

Figure 4. (**C**) Magnetization of blue-ordered regions with further cooling in same positive field, with self-reversed TRM. We postulate that blue regions magnetize compatibly across the few red APBs against red regions near (001), also with surrounding previously magnetized disordered matrix. The effect is that where blue ordered regions are separated by APBs, these all change to violet 0° APBs upon magnetization.

3.3 Requirements summary

Requirements for self-reversed TRM have been understood since the late 1950's, including the strong antiferromagnetic coupling between phases. A rhombohedral oxide intergrowth is required, consisting of a minor Fe-richer weakly ferrimagnetic ordered phase, with a higher Curie *T* and higher coercivity, together with a major Fe-poorer stronger ferrimagnetic ordered phase with a lower Curie *T* and lower coercivity. The minor ferrimagnetic phase magnetizes first at higher *T*, followed by magnetization of the more abundant more strongly ferrimagnetic phase at lower *T*. Because of the strong antiferromagnetic coupling, the abundant, more strongly ferrimagnetic phase, acquires self-reversed TRM.

The past trouble with the above requirements was finding a chemical process that allows them to occur. Based on our literature research and studies of a synthetic sample, including limited demonstration of self-reversal properties produced by annealing in Paper I (Fabian *et al.* 2011), and explanations of chemical evolution of intergrowths in Paper II (Robinson *et al.* 2012), we can now describe the possible or probable self-reversal process in four microstructure stages illustrated in Figs 3–6.

4 MAGNETIC INTERACTIONS IN SAMPLES WITH DIFFERENT COOLING HISTORIES

4.1 Microstructure stage 1

This is a quenched sample with a disordered host containing isolated Fe–Ti-ordered and Ti–Fe-anti-ordered domains of different sizes and compositions. When magnetized in the absence of a magnetic field, or in a very weak field, and with equal abundances of A-ordered and B-anti-ordered regions in a disordered host, it is possible that the A- and B-layer magnetizations will be equal and self-cancelling, giving a net magnetic moment of zero. A different situation likely applicable to our Ilm 61 sample (Fabian *et al.* 2011) produces a net ferrimagnetic moment with no evidence for self-reversal. In nature there could be a more or less accidental distribution at high *T* of slightly different A and B size regions. For simplicity of explanation, Fig. 3(A) shows only two sizes and they are displayed in a less than random pattern. The implication is that the smaller size regions, being less developed and less ordered, or being suppressed by coarsening of larger more ordered regions, contain more Fe^{3+} than the larger more-ordered size regions, and have a higher Curie *T*. As a result of this, red A and B regions with small arrows will magnetize first in a weak field directed to the right (Fig. 3B) followed at lower *T* by blue A and B regions with larger arrows (Fig. 3C). Blue A and B arrows all lie in parts of the crystal where small regions with red arrows and their surrounding disordered host have already been magnetized[1], so, in a weak field, they magnetize compatibly with the disordered host and at lower *T*.

More directly, when magnetizing in a magnetic field (Fig. 3B), in some parts of the material, red regions of A-ordering magnetize parallel to the field, thus orienting the moments of the adjacent disordered phase. Elsewhere red regions of B-anti-ordering magnetize first, thus orienting the moments of the adjacent disordered phase. The result of this is that magnetic domain walls (blue lines in Fig. 3B) will develop in the disordered antiferromagnetic host, separating regions where red A-ordered patches magnetized first, from regions where red B-anti-ordered patches magnetized first. Further at immediately lower *T* in the regions where red A-ordered areas magnetized first, blue B-anti-ordered areas will magnetize next. Similarly in regions where red B-anti-ordered areas were magnetized first, blue A-ordered areas will magnetize next. In a weak field, the blue areas will be forced to magnetize with sublattice magnetizations parallel to the host disordered phase, in the same p or q domain, but with a net ferromagnetic moment direction opposite from the red-ordered patches. The original blue magnetic domain walls of Fig. 3(B), remain in Fig. 3(C), and the configuration can explain a self-reversed TRM state.

Alternatively from Fig. 3(C), in a strong field, the blue areas will magnetize in the direction of the magnetic field (Fig. 3D; *cf*. Lagroix *et al.* 2004, Fig. 8). In the latter case, magnetization in the direction of the field will produce new blue magnetic domain walls in the host surrounding these B-ordered patches in a pattern different from Figs 3(B) and (C). Parallel processes will also happen to the A-ordered patches in the regions where B-ordered patches magnetized first. The result in Fig. 3(D), is a different, more complex and more abundant pattern of blue magnetic domain walls in the disordered host. Fig. 3(D) as compared to Fig. 3(C), shows a 54 per cent increase in abundance of domains walls, and hence a major increase in magnetic energy required to retain this state.

The following key messages concerning microstructure stage 1 come from Fig. 3. Fe-richer domains are much smaller than Ti-richer domains, and are separated by large volumes of the disordered phase. Thus, the small more Fe-rich regions magnetize first at higher *T*, followed at lower *T* by the larger more Ti-rich regions. AF coupling must take place entirely through the disordered phase. When first magnetized in a weak positive field, the intergrowth acquires a weak positive normal magnetization. At lower *T*, the antiferromagnetic coupling through the disordered phase would cause the majority phase to acquire a self-reversed (negative) magnetization. This process results in dividing the intergrowth into a complex array of 'p domains' and 'q domains' separated by purely magnetic domain walls in the disordered phase. Although self-reversal by coupling through the disordered matrix is not a certainty, it is a reasonable possibility, provided the larger Ti-rich regions are preponderant in terms of magnetic moment. When magnetized in a stronger field, the larger Ti-richer domains are reversed, and the pattern and abundance of magnetic domain walls is changed dramatically, with a consequent increase in energy. The p and q domains now contain purely A- and B-ordered regions, respectively.

4.2 Microstructure stage 2

After the sample was quenched, and then briefly annealed, it retains its extensive disordered host. This host is embedded with Fe–Ti ordered and Ti–Fe-anti-ordered domains of different sizes that have grown to impinge in a few places. This has led to local merging of some domains and limited development of antiphase and synphase boundaries.

The condition discussed here is illustrated in Fig. 4(A), where ordered regions start to impinge and create chemical APBs and CSPB, though disordered material is still abundant. In a weak field, magnetization occurs first in the diminished and more Fe-rich red A and B regions (Fig. 4B), giving a positive magnetic moment to

[1] We have, with some trepidation, ignored the possibility that the disordered host would magnetize at a slightly higher *T* than the red A-ordered and B-anti-ordered regions in a way incompatible with them. New experimental results and related inferences, too complex to give here, suggest this is improbable. Obviously this possibility would provide a further degree of chaos to the modeling.

the right in these small regions, and also providing a compatible magnetization to the disordered matrix. The magnetizations in the disordered matrix near the small red A regions, and the small B regions, have opposite sublattice orientations, therefore belong to p domains and q domains, respectively. The enlarged more Ti-rich A and B regions then magnetized at slightly lower T (Fig. 4C). In a weak field, their magnetization directions are not parallel to the field, but in directions compatible both with the surrounding disordered matrix, and with antiferromagnetic interactions in those few places along (001) where there are red CAPBs, which results in turning those boundaries into 180° CAPBs. The few orange synphase boundaries become 180° synphase boundaries. Where large blue A-ordered and blue B-anti-ordered domains have impinged diagonally, original red CAPBs without related magnetizations change, to violet 0° CAPBs. Under these circumstances, magnetic domain walls bordering ordered phases follow the orange 180° synphase boundaries and violet 0° APBs. Because enlarged A and B regions dominate the sample, their net magnetic moments suggest that such a sample would adopt a net negative magnetization and thus a self-reversed TRM (Fig. 4C). With more random natural domain sizes, placements, and boundaries, as compared to the rigid pattern here, there would be greater variety of details in the progress of impingement.

It is worth pointing out that the patterns of p and q domains are very similar in all the conceptual models purporting to show results from cooling in a weak positive magnetic field (Figs 3C, 4C, 5C, 6C below). That is because all the models started with an identical spatial array of centres of red and blue A-ordered and B-anti-ordered domains, and differ only in the degree of growth or shrinkage of domains. The same is true for the two models (Fig. 3D also 10B below) purporting to show cooling in or application of a very strong positive field.

4.3 Microstructure stage 3

The sample has been quenched and then annealed to the point where no disordered host remains. It consists entirely of an interlocking network of Fe–Ti-ordered and Ti–Fe-anti-ordered domains of different sizes and compositions separated by antiphase and synphase boundaries.

The condition following quench and annealing discussed here is illustrated in Fig. 5(A). This is the same as fig. 13(c) in Robinson *et al.* (2012). No disordered material is left, so that the sample consists entirely of ordered and anti-ordered domains separated by CAPBs and CSPBs. Fig. 5 gives a view of the progressive magnetization process of this microstructure stage similar to the progress shown in Figs 3 and 4, but with coarsening patterns that more closely mimic the patterns shown in the TEM images of Nord & Lawson (1989, 1992). Fig. 5(A) shows material that has coarsened to the point where there are no vestiges of the disordered phase save the thin layers required by contacts between ordered and anti-ordered phases as illustrated in Fig. 2(A).

In creating Fig. 5, chemical APBs were deliberately migrated away from blue A and B regions, making these larger, and toward red A and B regions making them smaller. Vestiges of the disordered phase have been eliminated along boundaries between phases with nearly identical ordering arrangements. For example, between red A regions, red B regions, blue A regions and blue B regions. Though there is no chemical antiphase relationship between red A and blue A, nor red B and blue B regions, they do differ in degree of chemical order and composition, and their mutual boundaries are marked as orange CSPB. The resulting patterns are remarkably similar to those produced in experiments by Nord & Lawson (1989), especially their Fig. 8. Their experiments prove that the CAPBs, with their postulated Fe-enrichment, are capable of substantial movement at high T, progressively eliminating the phase boundaries with greater annealing time and leading toward continuous volumes of a single ordered phase. The pattern shown in Fig. 5(A) may be but one of several stages, as suggested by Harrison (2006) in which finer patterns of intergrowths are incorporated into coarser patterns moving toward elimination of chemical boundaries.

The magnetic consequences of this pattern are shown in Figs 5(B) and (C). In the weak field of 5(B), the Fe-rich small A- and B-ordered domains magnetize ferrimagnetically parallel to the imposed field to the right, and immediately determine the pattern of p and q magnetic domains. The red A-ordered chemical domains control the p magnetic domains associated with yet unmagnetized blue B-ordered chemical domains, and the red B-ordered chemical domains control the q magnetic domains associated with yet unmagnetized blue A-ordered chemical domains. With further cooling, these associations exert control across the red CAPBs. Note that in Fig. 5(B) the p and q domain boundaries follow three kinds of chemical domain walls marked in different colours: (1) Red CAPBs between red A and blue B domains and red B and blue A domains only magnetized on one side. (2) Orange CSPBs between red A and blue A or red B and blue B domains, only magnetized on one side. (3) Violet 0° CAPBs between red A and red B magnetized regions. At this T stage the sample would be said to exhibit a weak normal TRM.

In the same weak field at lower T in Fig. 5(C), the blue B- and A-ordered chemical domains acquire a self-reversed magnetization magnetically compatible with their related p and q magnetic domains, respectively. This occurs by antiferromagnetic interaction across the predominant red CAPBs, which all become 180° CAPBs. The orange CSPBs are now magnetized on both sides and become 180° CSPB. The boundaries between blue A and B domains are also now magnetized on both sides and become 0° CAPBs, significantly extending the abundance of this type of boundary. At this T stage the sample would exhibit a strong self-reversed TRM.

It is important to see in Fig. 5(C) that, although the nature of the violet and orange boundaries creates a change from 0° to 180° in terms of magnetic moment orientation, this effect is caused by the presence of a continuous Bloch wall that follows the path between p and q domains defined by sublattice orientations. The different chemical nature of the boundaries causes the switch, but micromagnetically there is nothing controversial happening other than the presence of Bloch walls defined by the p–q boundary. These p–q boundaries contain a higher energy state than the 180° CAPBs contained entirely within p and q domains.

There is no scale to these conceptual models except in Fig. 2, where we know that a single cation layer is 0.23 nm thick and the entire model is ∼4.6 nm thick. It is an open question as to the degree of coarsening that can have taken place so the antiferromagnetic interactions across the CAPBs can be maintained, thus causing the blue anti-ordered domains to adopt a magnetization reversed relative to the red ordered domains. Similarly the critical size will depend to some extent on the strength of magnetizing field applied, as well as the magnetic configuration, for example the degree of Fe–Ti ordering in ferrimagnetic regions. Harrison *et al.* (2005) suggested that the negative magnetic exchange coupling between antiphase domains across 180° CAPBs appears to be easily overcome when APD (antiphase domain) size becomes greater than 50 nm, or about six times larger than we observed in our Ilm 61 sample or ten times thicker than the 20 cation layers shown in Fig. 2(A). This may allow

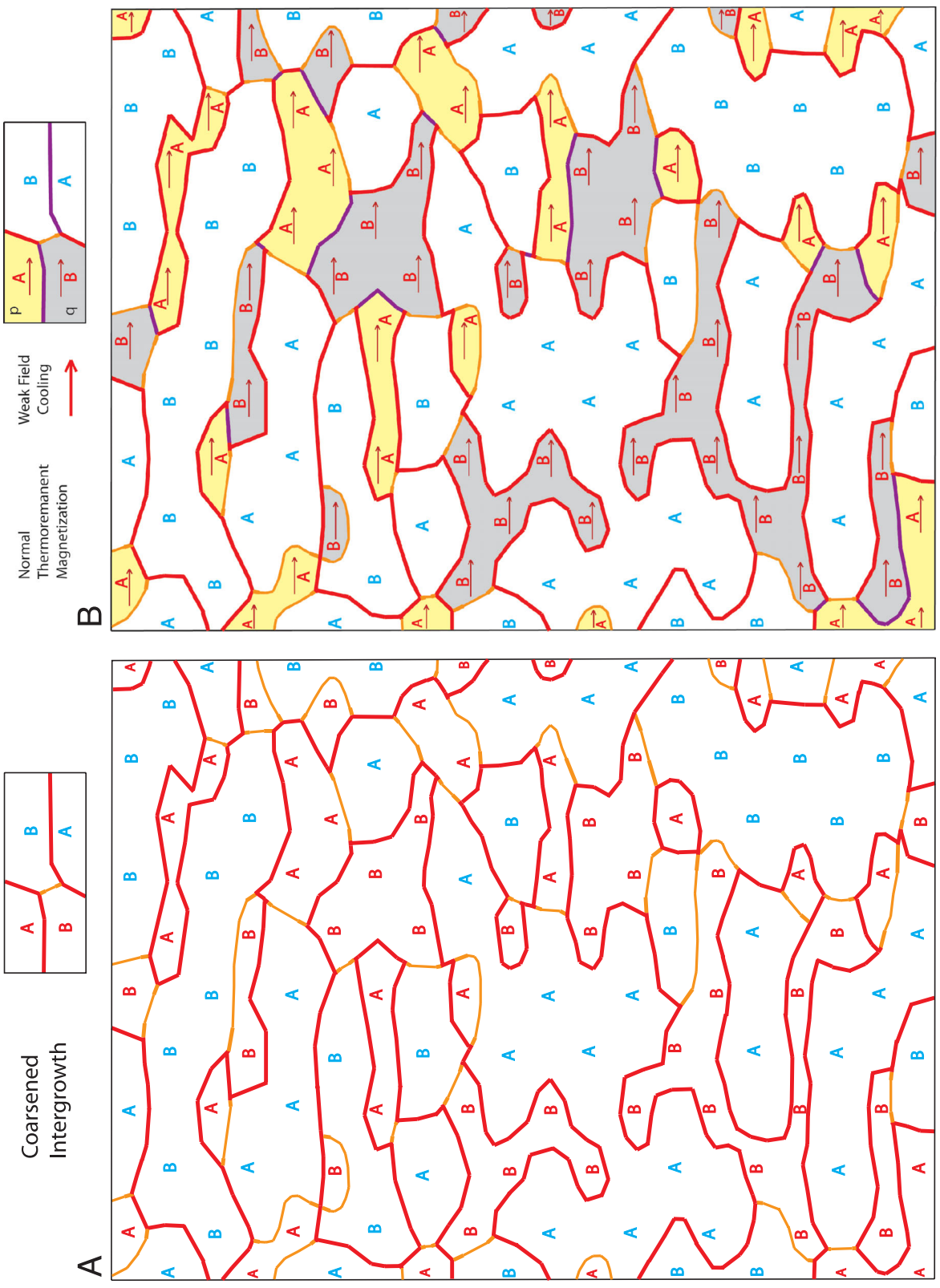

Figure 5. Sequence of acquisition of magnetization for microstructure stage 3 in weak positive field to right in coarsened intergrowth of ordered and anti-ordered domains with no disordered matrix remaining, except as required in phase-contact regions. **(A)** Coarsened intergrowth no disordered regions, leaving only red CAPBs and orange CSPBs. **(B)** Magnetization of red ordered domains in a positive field producing weak normal TRM. Where red A-ordered and red B-anti-ordered domains are adjacent, CAPBs (red) become 0° CAPBs (violet). Boundaries between red and blue domains are still not magnetic and remain as CAPBs and CSPBs. P and q domains are indicated in magnetized red domains, but not unmagnetized blue domains.

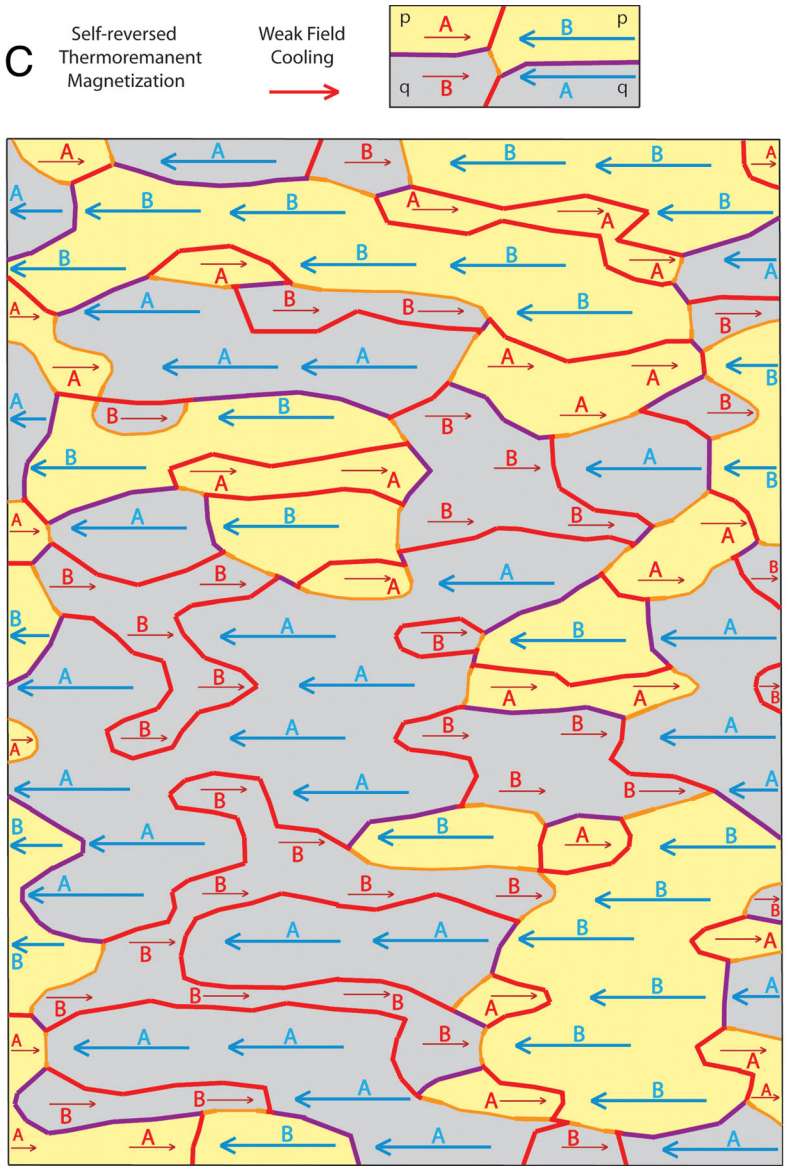

Figure 5. **(C)** Magnetization of blue-ordered domains with further cooling in same positive field, producing self-reversed TRM and causing more 180° CAPBs (red) to become 0° CAPBs (violet) along p–q domain boundaries. All CSPBs, become magnetic 180° CSPBs, all on p–q domain boundaries. More likely to result in self-reversed TRM than Fig. 3, because antiferromagnetic coupling occurs across thin CAPBs between ordered phases, not across disordered matrix. The 180° CSPBs may serve as locations to initiate field-induced magnetic re-orientation as in Fig. 10.

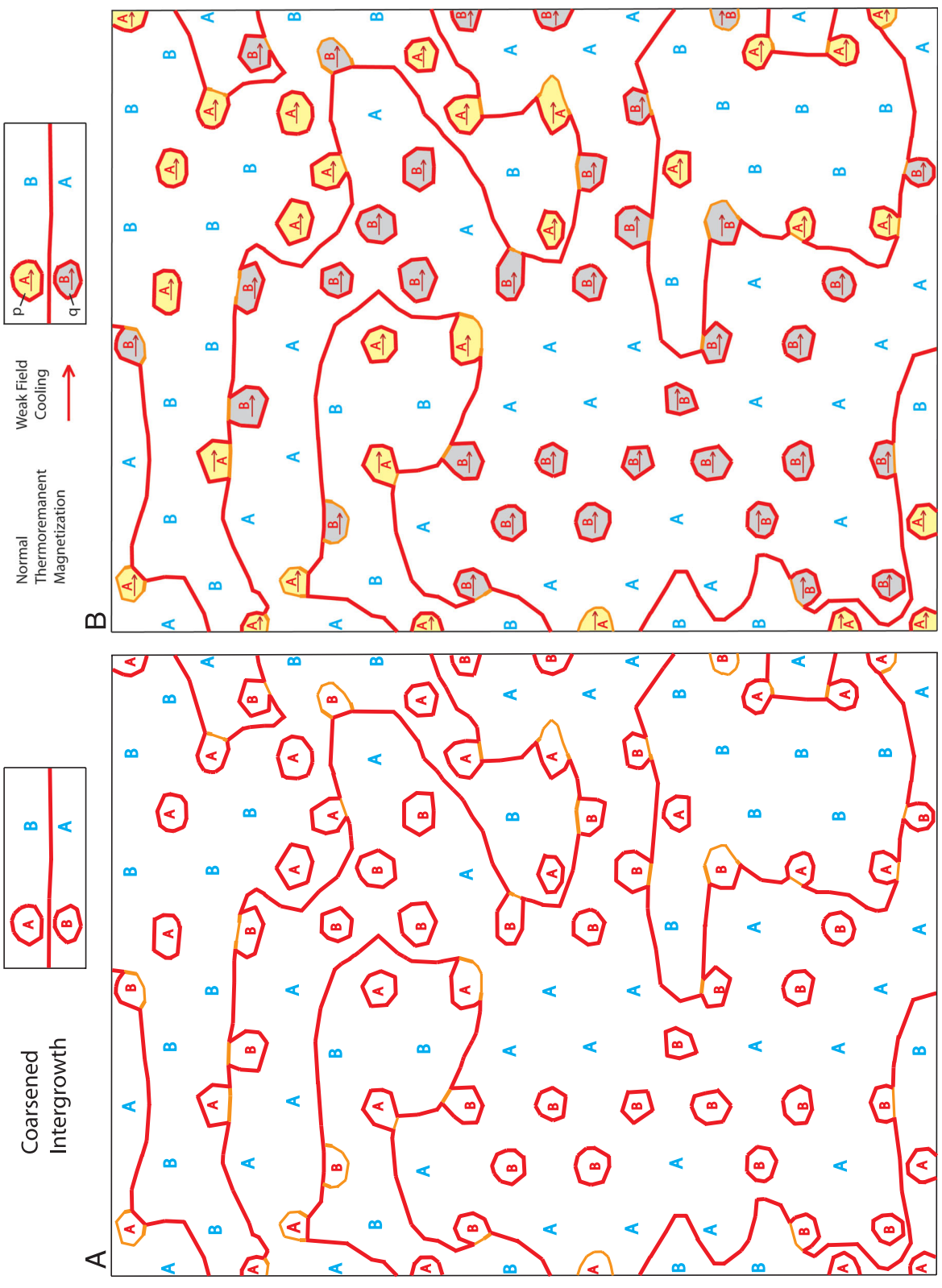

Figure 6. Sequence of acquisition of magnetization for microstructure stage 4 in weak positive field to right in coarsened intergrowth of ordered and anti-ordered regions. **(A)** No disordered matrix as in Figs 3 and 4. Small red ordered domains have shrunk while blue ordered domains have expanded and enveloped the small red domains. This agrees best with argument for Fe-enrichment in shrinking domains, but APB abundance may or may not be enough to provide postulated self-reversal. **(B)** Magnetization of isolated red-ordered regions in positive field producing a weak normal TRM. Red A-ordered domains belong to p domains and red B-anti-ordered domains belong to q domains, but there is no magnetic interaction across boundaries.

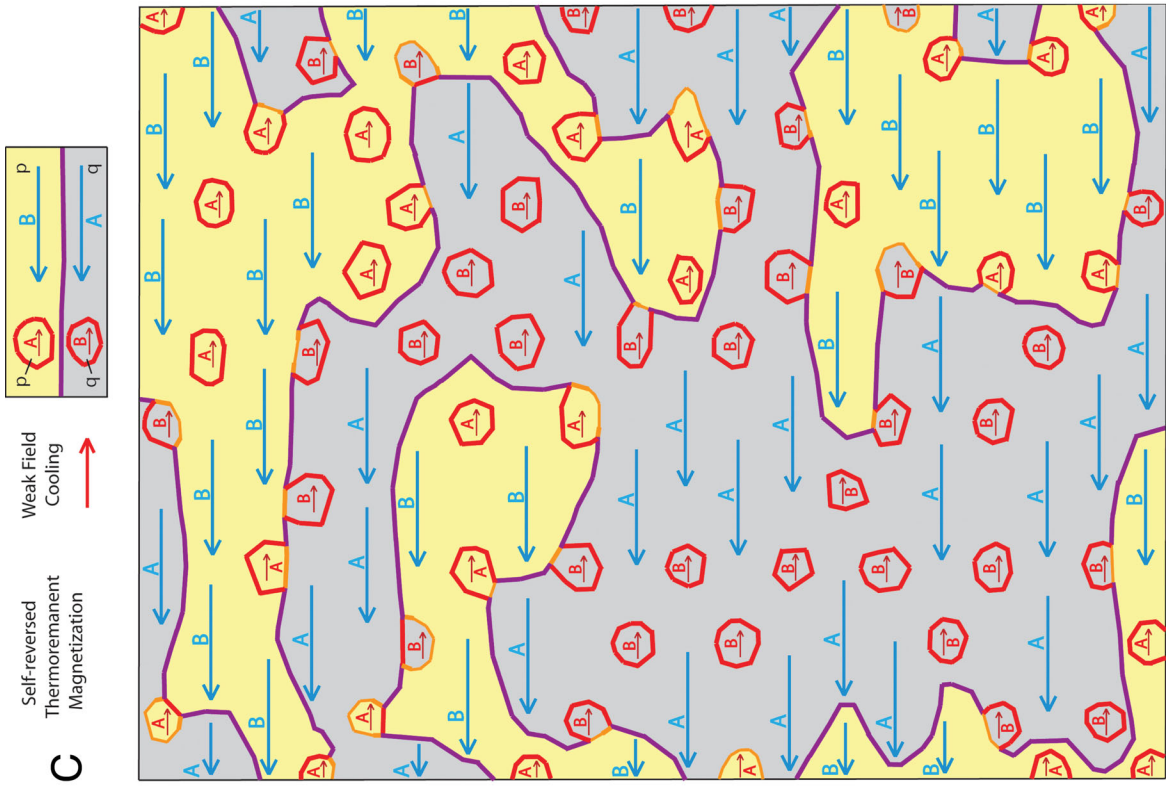

Figure 6. (**C**) Magnetization of blue-ordered regions with further cooling in same weak positive field. Blue domains are postulated to magnetize compatibly with adjacent previously magnetized red domains across abundant red 180° CAPBs. Model is divided into magnetically compatible p and q domains bounded by violet 0° CSPBs and orange 180° CSPBs.

only a small number of sequential coarsening cycles with magnetic consequences.

The following are key lessons concerning microstructure stage 3 to be taken from Fig. 5. All the disordered phase has been eliminated. Ordered and anti-ordered phases are bounded by CAPBs and CSPB. Here we can make the strongest argument that the small ordered domains are Fe-enriched and the large ordered domains are Ti-enriched. Further, without any disordered phase except for minor requirements related to contact layers, the situation is ideal for very strong 180º antiferromagnetic coupling across CAPBs. As such an intergrowth is magnetized, first with normal remanent magnetization and later with self-reversed magnetization, most of the CAPBs become the energetically favourable 180º CAPBs, but those on boundaries of between p and q domains, which are magnetic walls, become energetically unfavourable 0° CAPBs. All CSPBs lie on magnetic walls on bounding p and q domains and are energetically unfavourable 180º CSPBs.

4.4 Microstructure stage 4

The sample has been quenched and then annealed well beyond the point where a disordered host was eliminated. Instead, the large Fe–Ti-ordered and Ti–Fe-disordered domains have enlarged in a coarsening process at the expense of small domains, which have shrunk as well as becoming Fe-enriched. Further annealing would eliminate the smaller domains, resulting in a coarser intergrowth of larger domains.

The condition discussed here as stage 4 is illustrated in Fig. 6(A), a chemical progression from Fig. 5(A), produced during annealing. Here small red ordered and anti-ordered regions have decreased greatly in size and are now enveloped in larger and increasing blue ordered and anti-ordered regions. This drawing may contain at least one unnatural feature. The centres of the ordered regions were not permitted to migrate from their original positions, yet such migration is probably part of the natural coarsening process. This progression from Figs 5(A)–6(A) would lead, with further annealing, to elimination of small red regions and toward a coarser intergrowth of blue regions. Harrison (2006) suggested that at some larger scale, these blue domains could also show size differentiation, leading to second large-scale elimination of small regions and enlargement of large regions, leading ultimately, with the correct cooling history, to a single uniformly ordered phase. Boundaries between red and blue regions in Fig. 6(A) are dominantly CAPBs with a minority of CSPBs. Boundaries between blue regions are all CAPBs. The progression in Fig. 6(A) to the point where the small red ordered regions are greatly reduced in size, might provide the best conditions for postulated Fe enrichment, with consequent effects on magnetic properties. This pattern might also fit most closely with the abstract concepts of Uyeda (1958) and Ishikawa & Syono (1963), in which the small red ordered and anti-ordered regions would play the role of the ‘x phase’.

Fig. 6 gives a view of the progressive magnetization process similar to the progress shown in Fig. 5, but with coarsening patterns that appear to go beyond those shown in TEM images by Nord & Lawson (1989, 1992). The magnetic results are crudely similar. The magnetic consequences of the pattern in Fig. 6(A) are shown in Figs 6(B) and (C). In the weak field of 6(B), the Fe-rich small A- and B- ordered domains magnetize parallel to the imposed field to the right. This determines the pattern in which red A-ordered chemical domains control the p magnetic domains associated with unmagnetized blue B-ordered chemical domains, and the red B-ordered chemical domains control the q magnetic domains associated with unmagnetized blue A-ordered chemical domains. At this T stage the sample would exhibit a weak normal TRM.

With further cooling in a weak field as shown in Fig. 6(C), this control will eventually be exerted across the red CAPBs, turning them into 180° CAPBs, and in the process compatibly magnetizing the blue A-ordered and B-anti-ordered domains. In this process small sections of orange CSPBs will become 180° CSPBs on borders where red A and blue A, or red B and blue B domains impinge. In addition, CAPBs on borders between blue A ordered and blue B anti-ordered domains will become violet 0° CAPBs. In Fig. 6(C) the p and q domain boundaries, follow two kinds of chemical domain boundaries, orange 180° CSPBs and violet 0° CAPBs. At this T stage the sample would exhibit a strong self-reversed TRM.

The following key lessons concerning microstructure stage 4 come from Fig. 6. It represents an additional stage in the coarsening process compared to stage 3 in Fig. 5. Here small domains have become even smaller and possibly more Fe-rich and are enveloped in much larger coarsening regions of Ti-rich domains, that would lead, with further annealing, to an intergrowth with only large domains remaining. Initial positive magnetization of the small Fe-rich domains divides the sample into isolated p and q domains, with opposite sublattice magnetizations, enveloped in a non-magnetic matrix. When the large Ti-rich domains magnetize at lower T, they respond antiferromagnetically across the CAPBs surrounding the small Fe-rich domains and adopt a self-reversed magnetization. In this process, the boundaries between large Ti-rich regions change from non-magnetic CAPBs to 0° CAPBs, and CSPBs change to 180° CSPBs, both becoming magnetic walls between p and q sublattice domains.

5 MECHANISM FOR ROOM-T MAGNETIC EXCHANGE BIAS AND APPLICATION

5.1 Historical background

The presence of positive room-T exchange bias was illustrated by Meikeljohn & Carter (1959), for a sample of composition Ilmenite 60. Their measurements, redrawn in Fig. 7, emphasize that the observed bias results from exchange coupling and not from a vertical shift of the loop. This is seen by studying the vertical difference between the hysteresis branches in Fig. 7, which is considerably asymmetric, with an excess at positive field values of 3–6 kOe. A similar result is also illustrated in diagrams of the hysteresis of remanence for compositions Ilmenite 51 (Fig. 8) and Ilmenite 46.5 (Fig. 9) by Ishikawa & Syono (1963). None of these experiments attained saturation by application of strong enough fields, and the remanent magnetizations measured in Figs 8 and 9 do not yield conventional hysteresis loops. In all three cases, these samples show self-reversed TRM acquired in a positive cooling. They also appear to show positive magnetic exchange bias. We explore this relationship in the conceptual model in Fig. 10.

5.2 Graphic model

Fig. 10 illustrates the progressive effects of applying a strong positive field to a sample initially containing a self-reversed TRM as already shown in Fig. 5(C). By that stage, with only ordered and anti-ordered domains magnetized by cooling in a weak field, there are two types of CAPBs: red 180° CAPBs within areas of p domains or q domains; and violet 0° CAPBs along boundaries between p and q

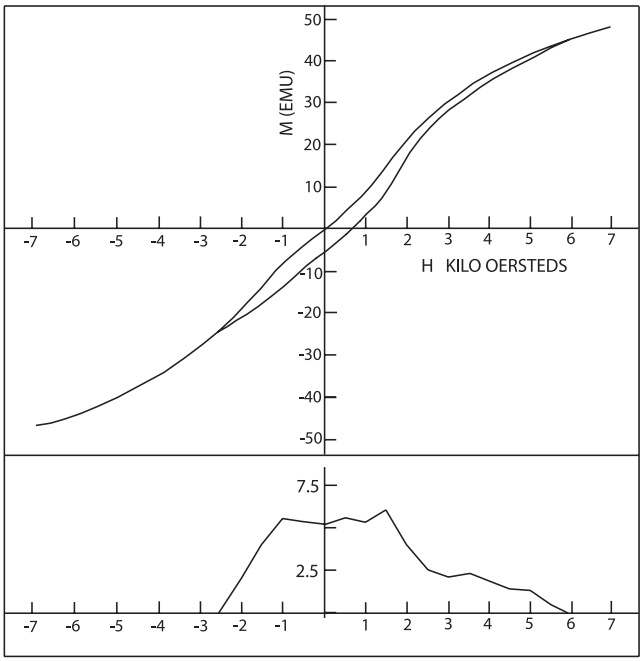

Figure 7. The first magnetization curve shown to exhibit positive exchange bias reported for synthetic Ilmenite 60 by Meikeljohn & Carter (1959). The sample was cooled in a positive field of 10 000 Oersted from 500°C to room *T*, and measured at room *T*. Sample was chosen to be similar to composition in Haruna Dacite for which Uyeda (1958) put forward an exchange-coupling model for magnetic self reversal. Meikeljohn & Carter (1959) reported positive loop shift of 350 Oe. Our lower plot of difference between two hysteresis branches indicates the asymmetric part of the loop extends to 6000 Oe. Except for the lower plot, this is a retracing of a historical figure, and the scales were not converted to SI units.

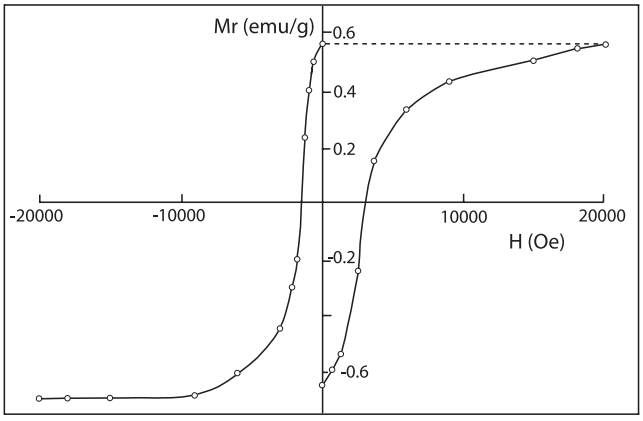

Figure 8. Ishikawa & Syono (1963) measured hysteresis of remanence for sample with composition Ilmenite 51 that also showed self-reversed TRM. Following quench, it was annealed 20 min at 600 °C, then cooled in a field of +100 Oe from 450 °C, whereby it acquired negative remanence. Successive application of increasing positive fields up to +20000 Oe changed remanence from –0.64 to +0.56 emu g^{-1} and thus is not able to completely reverse the self-reversed TRM. In contrast, later application of increasingly larger negative fields reversed the remanence much faster to −0.69 emu g^{-1}—even beyond its initial value. This again indicates presence of an irreversible magnetic component with very high coercivity. On this is retracing of a historical figure the scales were not converted to SI units.

domains. There are also 180° CSPBs along the boundaries between p and q domains. In the case of the CSPBs, the 180° relationship means that the CSPBs are locations of energetically unfavourable magnetic p–q domain walls. As the strong positive field is applied (Fig. 10A) the edges of the self-reversed blue A and B domains begin to acquire a positive magnetization. This begins first along the orange 180° CSPBs converting them quickly to green 0° CSPBs, as soon as the associated p–q domain walls move into the adjacent blue domains. From these locations blue 180° magnetic p–q domain walls migrate across the blue ordered and anti-ordered domains, conspicuously lengthening these energetically unfavourable walls and creating new domain patterns. Lengthening the walls creates considerable resistance to the reversal of magnetization in the blue domains from negative to positive. Increased positive magnetic field causes further migration and lengthening with increasing resistance offered. This is the situation portrayed and achieved experimentally by Ishikawa & Syono (1963) in an annealed sample of Ilm 46.5 by application of a field of 1.4 Tesla (Fig. 9 above).

Application of a stronger field (Fig. 10B) should eventually move all the blue 180° magnetic domain walls of Fig. 10(A) until they collide with all the red 180° CAPBs turning them, without exception, into violet 0° CAPBs. At this point, with all chemical domains showing a positive magnetization, all their boundaries are either violet 0° CAPBs, that are magnetic walls on p–q domains boundaries, or green 0° CSPBs which are no longer magnetic walls. The violet walls are the only magnetic walls in Fig. 10(B) and they work against normal antiferromagnetic coupling between domains. Comparisons of Figs 5(C) and 10(B) shows that energetically unfavourable magnetic walls are approximately 67 per cent more abundant and much longer in 10(B) than in 5(C), explaining why a very strong field would be needed to attain and maintain this saturated state. The high energy of this saturated state, with much greater domain wall length compared to the self-reversed state, is a requirement for exchange bias.

It is logical that the energetically unfavourable boundaries, either 0° CAPBs, or surficially more abundant 180° magnetic domain walls are fairly quickly reduced with imposition of a weak negative field. Ishikawa & Syono (1963) achieved this with a negative field of 0.1 Tesla (Fig. 9). Such a demagnetization is also illustrated in fig. 1 of Harrison *et al.* (2005) where an initial strong field (in this case negative) of 1000 mT, producing a nearly pervasive negative magnetization, was followed by progressive weak positive fields of 1.9 mT, 10.6 mT and 12.8 mT. The end product was a material dominated by a positive magnetization essentially equivalent to the self-reversed state. Further, their holographic image shows magnetic changes across chemical boundaries and also migration of 180° magnetic walls, similar to the behaviour simulated in Figs 10(A) and (B).

Although we do not illustrate it here, one needs to consider a state beyond the demagnetization in a weak negative field just described. What could happen in an extreme negative field would be reversal of the positive magnetic moments of the Fe-rich red A- and B-anti-ordered domains. Ishikawa and Syono do not illustrate this, probably considering such material (their 'x phase') to have a very high coercivity closely allied to that of a disordered host. It is probable that such a condition will be hard to reach because the weak ferrimagnetization in this material must overcome the very strong antiferromagnetic coupling with the very much larger and more strongly magnetized Fe-poor blue A-ordered and B-anti-ordered domains. If achieved, the result would be a pattern of magnetic domains exactly opposite from those in Fig. 10(B), with the same abundant violet 0° CAPBs, but with p domains and q domains

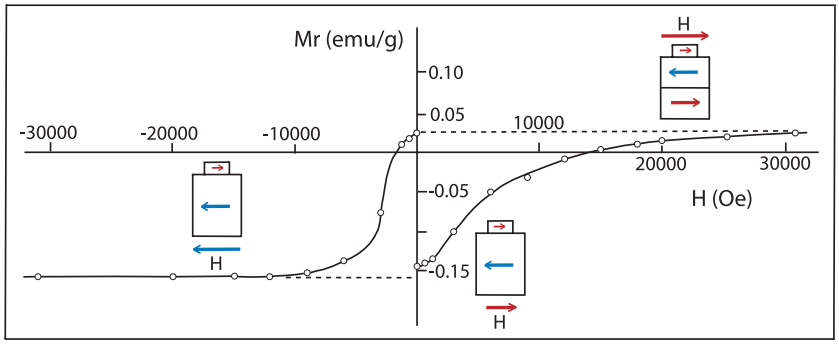

Figure 9. Even more pronounced bias than in Fig. 8 observed by Ishikawa & Syono (1963) for sample with composition Ilmenite 46.5 that also shows self-reversed TRM. The experimental conditions were same as in Fig. 8. Ishikawa & Syono (1963) point out that coercivity of remanence for positive field is $H_{cr+} > 14000$ Oe, while the field necessary to remove final positive remanence is only about $H_{cr-} > 1000$ Oe. Three sketched boxes indicate their explanation by approximate proportions of positive (right-hand side) and negative (left-hand side) magnetizations in weak negative and strong positive fields. The central sketch, added by us, shows condition of self-reversed magnetization. The magnetic moment arrows in the sketched boxes are coloured red if positive, blue if negative. Our interpretation only adds a detailed process to the generally correct explanation of Ishikawa & Syono (1963). In a strong positive field some of the large box gains a positive magnetization (blue arrow changes to red) by overcoming the strong antiferromagnetic coupling across CAPBs. Small red regions are considered to be more Fe-rich, less ordered, and magnetically hard, so that no negative field applied in this experiment was strong enough to change their magnetizations from positive to negative. On this is retracing of a historical figure the scales were not converted to SI units.

exactly switched If such a state could be reached, there is no guarantee that a return to a weak positive field would be able to re-establish the self-reversed state as in Fig. 5(C).

5.3 Summary of exchange bias arguments

The possibility for room-*T* magnetic exchange bias in this composition range was demonstrated as far back as 1959. The process begins with acquisition of self-reversed (negative) TRM in a weak positive field. When a stronger positive field is applied, the larger negatively magnetized domains begin to reverse. This process is initiated along the energetically unfavourable 180° CSPBs that are magnetic walls, and converting them into 0° CSPBs, which are not magnetic walls. The process continues as purely magnetic domain walls move into the negatively magnetized ordered domains converting them progressively to positively magnetized. As the magnetic domain walls move across the ferrimagnetic ordered domains, they lengthen dramatically, increasing the resistance to further movement. This movement reaches a limit when the magnetic domain walls impinge on the 180° CAPBs that are not magnetic walls, converting them all to 0° CAPBs, which are magnetic walls. This magnetically saturated state has been achieved in holography results (Harrison *et al.* 2005), but may be restricted when the antiphase domains are <50 nm wide.

When the strong field is decreased, all the above complexities disappear easily, likely returning the sample to the 'relaxed' self-reversed state while the field is still weakly positive. Application of progressively stronger negative fields probably does little to change the features of the self-reversed state, and there is some question how strong a negative field would be needed to begin reversing the small Fe-rich initially positively magnetized domains (Shcherbakov *et al.* 2009). Thus, following conditions of acquisition of self-reversed TRM in a weak positive magnetic field, the magnetic exchange bias should show a positive shift. Furthermore, the intergrowth conditions for both self-reversal and exchange bias are similar. In magnetic holography experiments on an Ilm 70 sample with a CAPB intergrowth, Harrison *et al.* (2005) achieved both positive and negative saturated states, creating 0° CAPBs. We suspect that this sample contained too few domains small enough to resist this saturation, consistent with the implication that small domain size is a key to both properties.

Although the chemical-magnetic models presented in this paper qualitatively show how the properties of self-reversed TRM and positive room-*T* magnetic exchange bias can develop, a large series of experiments involving different quench and annealing conditions on phases of varied composition will be needed to identify intergrowths that will produce these properties best. In this solid solution, the largest exchange bias ever measured was in an AF host (titanohematite) with nanometer-sized ilmenite lamellae (Harrison *et al.* 2007; McEnroe *et al.* 2007). This exchange was only present below the magnetic ordering T of the ilmenite at <57 K. The Fe contact layers presumed to be present in that material are similar to the contact layers between the AF and FM phases described here.

6 DIRECTION OF FUTURE RESEARCH

The chemical-magnetic conceptual models given here describe what likely happens during acquisition of self-reversed TRM and positive room-*T* magnetic exchange bias. They do not provide accurate information on which conditions of quench and annealing will provide the intergrowths in which these properties are optimized. That information can only be provided by a large series of experiments involving different quench and annealing conditions on phases of varied composition. A first step in this direction, including cooling curves in both low and high fields, was provided by Lagroix *et al.* (2004). Initial identification will be magnetic, followed by TEM studies where relative domain sizes and positions can be observed. We are presently well embarked on such a program and have found good magnetic evidence for very significant Fe-enrichment of phase boundaries and Fe-depletion of ordered domains, already anticipated by Harrison (2006). These produce a surprising fine structure in acquisition of self-reversed TRM that will be described in a future publication. The new findings do not violate any of the principles and nomenclature used here.

7 CONCLUSIONS

The key to understand self-reversed TRM and room-*T* magnetic exchange bias lies in the antiferromagnetic interaction between

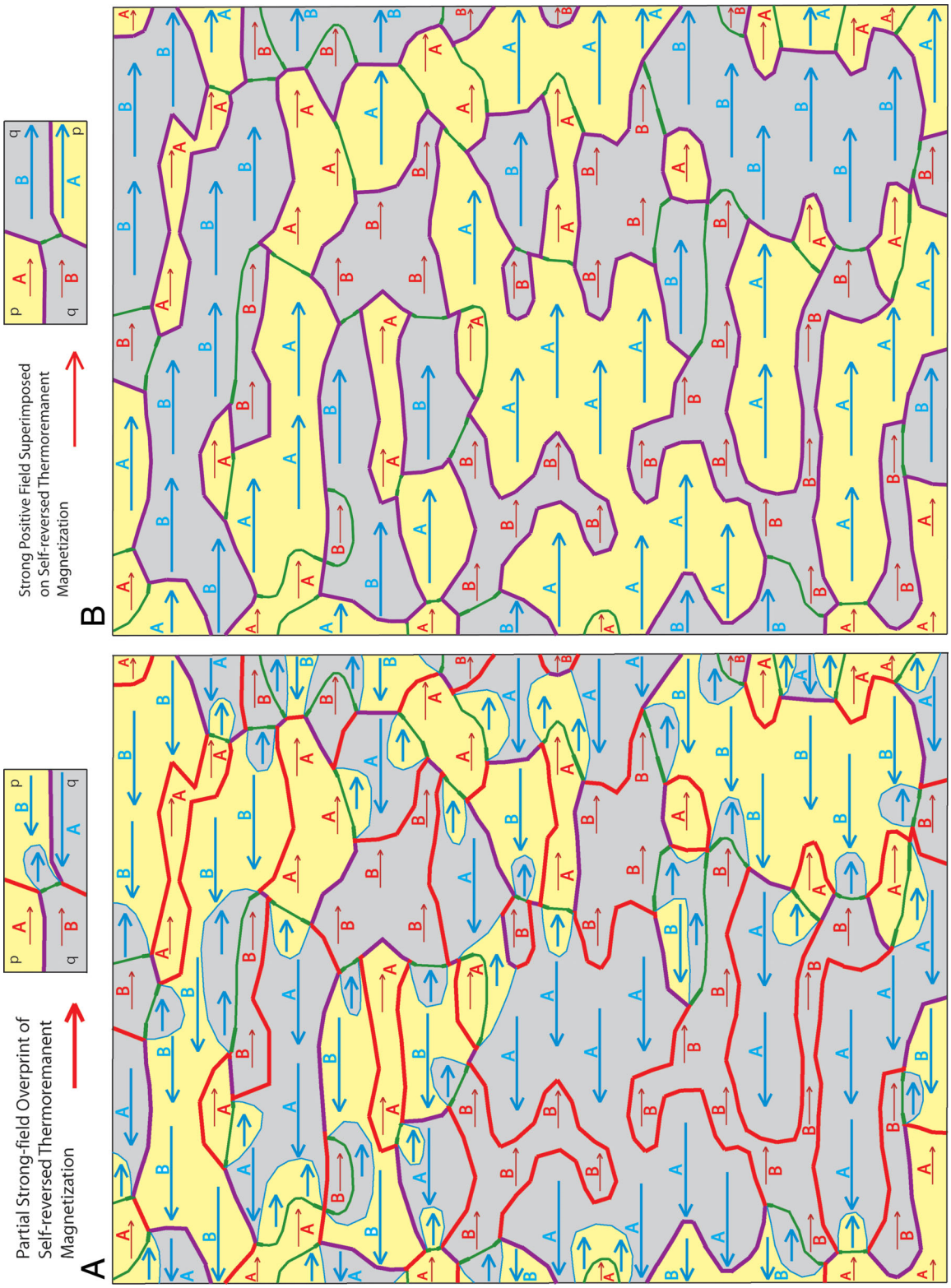

Figure 10. Illustration of effects of applying very strong positive field to a sample of microstructure stage 3 initially demonstrating self-reversed TRM. Consideration of three-step progression requires examination of the self-reversed state in Fig. 5(C), not repeated here. There, CAPBs include red 180° type within p and q domains, and also violet 0° type along the p–q domain boundaries. CSPBs are all orange 180° type also along p–q domain boundaries. (A) Early stage in application of very strong positive field. All self-reversed blue A-ordered and B-anti-ordered domains begin to acquire positive magnetization. This is initiated along CSPBs, particularly favourable for beginning this induced reversal. They undergo widespread change from orange 180° CSPBs on magnetic walls to green 0° CSPBs not on magnetic walls. Here 180° purely magnetic domain walls (thin blue lines) migrate through ordered and anti-ordered ferrimagnetic phases. Increasing magnetic domain wall length causes increasingly strong resistence to superimposed normal magnetization, even though the magnetization itself increases dramatically. (B) Ultimate limit of this process, possibly not attainable in some samples in normal instrumental fields. All magnetic domain walls have moved and expanded until impinged on chemical APBs, so that all domains show positive magnetization. All red 180° CAPBs, which are not magnetic walls in 5C, become violet 0° CAPBs that are magnetic walls in 10B, and magnetic wall length has increased ~67 per cent from 5C to 10B. We do not illustrate situation where a strong negative field might reverse small red ordered domains. This is less likely (and may be impossible depending on domain size) because of higher Fe-content, lesser order and magnetic hardness of these small domains, which, to attain a negative magnetization, must overcome strong coupling with adjacent larger blue domains.

alternating cation layers. This interaction must be exerted in fine-grained intergrowths produced in ferri-ilmenite solid solutions that have been quenched above their Fe–Ti ordering *T*s, partially ordered under metastable conditions during quench, and then, most commonly, annealed for a short time at *T*s below the ordering *T*. The best combination and sequence of *T* conditions will produce material with small A-ordered and B-anti-ordered regions that are more Fe-rich, less ordered, and have higher magnetization *T*s, embedded between and within larger A-ordered and B-ordered regions that are less Fe-rich, more ordered, and have a lower magnetization *T*. A key feature of these compositions is that all chemical processes are completed at *T*s well above the *T*s where magnetization begins, so that chemical evolution and magnetic evolution can be considered separately, even though the consequences of chemical development are absolutely crucial to magnetic development.

Here we have studied the progressive magnetization of four different stages in microstructure evolution. For each stage, we proposed a sequence of acquired magnetization in which small Fe-enriched domains magnetize first at higher *T* followed by acquisition of self-reversed TRM at lower *T*. We do not yet know which of these stages provides the best arrangement for self-reversed magnetization, but each presents a scenario by which it could take place and the magnetic interactions involved in each are explained in detail. The microstructures before magnetization include boundaries between disordered and ordered phases, and chemical antiphase and synphase domain boundaries between ordered phases. Magnetization acquisition involves moving magnetic walls, and chemically fixed 180° antiphase domain boundaries and 180° synphase domain boundaries evolving in stronger fields to 0° antiphase domain boundaries and 0° synphase domain boundaries, all described in detail. In terms of microstructures, already observed many years ago in TEM images of samples known to provide self-reversal, the third of the four stages is likely the most promising. Using the self-reversed state of this model material, we have then presented a conceptual model of how this microstructure may also explain room-*T* magnetic exchange bias.

ACKNOWLEDGMENTS

The research related to this series was supported by grant 189721 from the Research Council of Norway (Nanomat Program) in the EU Matera Program, and visiting fellowships to the Institute of Rock Magnetism, which is supported by an NSF Instruments and Facilities Grant. Significant manuscript preparation took place while Robinson and McEnroe were resident at BGI, Bayreuth, where McEnroe held an EU Marie Curie Fellowship 2009–2010 in cooperation with Prof. Falko Langenhorst. Their earlier work at Bayreuth was also supported by an EU Access to Infrastructures Grant. The manuscript was improved by precise notes and useful suggestions from France Lagroix and an anonymous reviewer. To each of these persons and institutions we extend our grateful acknowledgement.

REFERENCES

Burton, B.P., Robinson, P., McEnroe, S.A., Fabian, K. & Boffa Ballaran, T., 2008. A low-temperature phase diagram for ilmenite-rich compositions in the system Fe_2O_3-$FeTiO_3$, *Am. Mineral.,* **93,** 1260–1272.

Fabian, K., McEnroe, S.A., Robinson, P. & Shcherbakov, V.P., 2008. Exchange bias identifies lamellar magnetism as the origin of the natural remanent magnetization in titanohematite from ilmenite exsolution, Modum, Norway, *Earth planet. Sci. Lett.,* **268,** 339–353.

Fabian, K., Miyajima, N., Robinson, P., McEnroe, S.A., Boffa Ballaran, T. & Burton, B.P., 2011. Chemical and magnetic properties of rapidly cooled metastable ferri-ilmenite solid solutions: implications for magnetic self-reversal and exchange bias—I. Fe-Ti order transition in quenched synthetic Ilm 60, *Geophys. J. Int.,* **186,** 997–1014.

Harrison, R.J., 2006. Microstructure and magnetism in the ilmenite-hematite solid solution: a Monte Carlo simulation study, *Am. Mineral.,* **91,** 1006–1023.

Harrison, R.J. & Becker, U., 2001. Magnetic ordering in solid solutions, *EUR. Mineral. Union Notes Min.,* **3,** 349–383.

Harrison, R.J. & Redfern, S.A.T., 2001. Short- and long-range ordering in the ilmenite-hematite solid solution, *Phys. Chem. Minerals,* **28,** 399–412.

Harrison, R.J., Kasama, T., White, T.A., Simpson, E.T. & Dunin-Borkowski, R.E., 2005. Origin of self-reversed thermoremanent magnetization, *Phys. Rev. Lett.,* **95,** 268501, doi:10.1103/PhysRevLett.95.268501.

Harrison, R.J., McEnroe S.A., Robinson, P., Carter-Stiglitz, B., Palin, E.J. & Kasama, T., 2007. Low-temperature exchange coupling between Fe_2O_3 and $FeTiO_3$: insight into the mechanism of giant exchange bias in a natural nanoscale intergrowth, *Phys. Rev. B,* **76,** 174436, doi:10.1103/PhysRevB.76.174436.

Hofmann, K.A., 1975. Cation diffusion processes and self-reversal of thermoremanent magnetization in the ilmenite-hematite solid solution series, *Geophys. J. R. astr. Soc.,* **41,** 331–337.

Hoffman, K.A., 1992. Self-reversal of thermoremanent magnetization in the ilmenite-hematite system: order-disorder, symmetry and spin alignment, *J. geophys. Res.,* **97,** 10883–10895.

Hoffman, V. & Fehr, K.Th., 1996. Micromagnetic, rockmagnetic and mineralogical studies on dacitic pumice from the Pinatubo eruption (1991, Philipines) showing self-reversed TRM, *Geophys. Res. Lett.,* **23,** 2835–2838.

Ishikawa, Y., 1958. An order-disorder phenomenon in the $FeTiO_3$-Fe_2O_3 solid solution series, *J. Phys. Soc. Japan,* **13,** 838–837.

Ishikawa, Y. & Syono, Y., 1963. Order-disorder transformation and reverse thermo-remanent magnetism in the $FeTiO_3$-Fe_2O_3 series, *J. Phys. Chem. Solids,* **24,** 517–528.

Ishikawa, Y., Saito, N., Arai, M., Watanabe, Y. & Takei, H., 1985. A new oxide spin glass system of (1-x) $FeTiO_3$ – x Fe_2O_3. I. Magnetic Properties, *J. Phys. Soc. Japan,* **54,** 312–325.

Lagroix, F., Banerjee, S.K. & Moskowitz, B.M., 2004. Revisiting the mechanism of reversed thermoremanent magnetization (rTRM) based on observations from synthetic ferrian ilmenite ($y = 0.7$), *J. geophys. Res.,* **109,** B12108, doi:10.1029/2004JB003076.

McCammon, C., McEnroe, S.A., Robinson, P. & Burton, B.P., 2009. Mössbauer spectroscopy used to quantify natural lamellar remanent magnetization in single-grains of ilmeno-hematite, *Earth planet. Sci. Lett.,* **288,** 268–278.

McEnroe, S.A., Carter-Stiglitz, B., Harrison, R.J., Robinson, P., Fabian, K. & McCammon, C., 2007. Magnetic exchange bias of more than 1 Tesla in a natural mineral intergrowth, *Nat. Nanotechnol.,* **2,** 631–634.

Meiklejohn, W.H. & Carter, R.E., 1959. Exchange anisotropy in rock magnetism, *J. appl. Phys.,* **30,** 2020.

Nabi, H.S., Harrison, R.J. & Pentcheva, R., 2010. Magnetic coupling parameters at an oxide-oxide interface from first principles: Fe_2O_3-$FeTiO_3$, *Phys. Rev. B,* **81,** 214432, doi:10.1103/PhysRevB.81.214432.

Nord, G.L., Jr. & Lawson, C.A., 1989. Order-disorder transition-induced twin domains and magnetic properties in ilmenite-hematite, *Am. Mineral.,* **74,** 160–176.

Nord, G.L., Jr. & Lawson, C.A., 1992. Magnetic properties of ilmenite 70-hematite 30: effect of transformation-induced twin boundaries, *J. geophys. Res.,* **97,** 10 897–10 910.

Prévot, M., Hoffman, K.A., Goguitchaichvili, A., Doukhan, J-C., Shcherbakov, V. & Bina, M., 2001. The mechanism of self-reversal of thermoremanence in natural hemoilmenite crystals: new experimental data and model, *Phys. Earth planet. Inter.,* **126,** 75–92.

Robinson, P., Harrison, R.J., McEnroe, S.A. & Hargraves, R., 2002. Lamellar magnetism in the hematite-ilmenite series as an explanation for strong remanent magnetization, *Nature,* **418,** 517–520.

Robinson, P., Harrison, R.J., McEnroe, S.A. & Hargraves, R., 2004. Nature and origin of lamellar magnetism in the hematite-ilmenite series, *Am. Mineral.,* **89,** 725–747.

Robinson, P., Fabian, K. & McEnroe, S.A., 2010. The geometry of ionic arrangements and magnetic interactions in ordered ferri-ilmenite solid solutions and its effect on low-temperature magnetic behavior, *Geochem. Geophys. Geosyst.,* **11,** Q05Z17, doi:10.1029/2009GC002858.

Robinson, P., Harrison, R.J., Miyajima, N., McEnroe, S.A. & Fabian, K., 2012. Chemical and magnetic properties of rapidly cooled metastable ferri-ilmenite solid solutions: implications for magnetic self-reversal and exchange bias—II. Chemical changes during quench and annealing, *Geophys. J. Int.,* **188,** 447–472, doi:10.1111/j.1365-246X.2011.05277.x.

Shcherbakov, V.P., Fabian, K. & McEnroe, S.A., 2009. A mechanism of exchange bias for nanoparticles embedded in an antiferromagnetic matrix, *Phys. Rev. B,* **80,** 174419, doi:10.1103/PhysRevB.80.174419.

Uyeda, S., 1957. Thermo-remanent magnetism and coercive force of the ilmenite-hematite series, *J. Geomag. Geoelectr.,* **9,** 61–78.

Uyeda, S., 1958. TRM as a medium of paleomagnetism, with special reference to reverse thermo-remanent magnetism, *Japan J. Geophys.,* **2,** 1–123.